NASA TR R-103

NATIONAL AERONAUTICS AND SPACE ADMINISTRATION

TECHNICAL REPORT
R-103

THEORETICAL ELASTIC STRESS DISTRIBUTIONS ARISING FROM DISCONTINUITIES AND EDGE LOADS IN SEVERAL SHELL-TYPE STRUCTURES

By ROBERT H. JOHNS and THOMAS W. ORANGE

1961

For sale by the Superintendent of Documents, U.S. Government Printing Office, Washington 25, D.C. Yearly subscription, $15; foreign, $19.00; single copy price varies according to size ..... Price 45 cents

TECHNICAL REPORT R-103

THEORETICAL ELASTIC STRESS DISTRIBUTIONS ARISING FROM DISCONTINUITIES AND EDGE LOADS IN SEVERAL SHELL-TYPE STRUCTURES

By ROBERT H. JOHNS and THOMAS W. ORANGE

Lewis Research Center
Cleveland, Ohio

CONTENTS

TECHNICAL REPORT R-103

THEORETICAL ELASTIC STRESS DISTRIBUTIONS ARISING FROM DISCONTINUITIES AND EDGE LOADS IN SEVERAL SHELL-TYPE STRUCTURES

By Robert H. Johns and Thomas W. Orange

SUMMARY

The deformation and complete stress distribution are determined for each of the following edge-loaded thin shells of revolution: (1) a right circular cylinder, (2) a frustum of a right circular cone, and (3) a portion of a sphere. The locations of the maximum circumferential and meridional stresses on both the inner and outer surfaces are also found. The basic equations for the above were selected from the published literature on the subject and expanded to produce resultant-stress equations in closed form where practicable to do so. Equations are also developed for the discontinuity shear force and bending moment at each of the following junctions: (1) axial change of thickness in a circular cylinder, (2) axial change of thickness in a cone, (3) change of thickness in a portion of a sphere, (4) a cylinder and a cone, (5) a cylinder and a portion of a sphere, (6) a cylinder and a flat head, and (7) a cone and a portion of a sphere.

INTRODUCTION

Weight considerations in space-flight structures require loading or stressing of the structures very nearly to their maximum capabilities. It is therefore important that the operating stresses be known with a high degree of accuracy. With this knowledge it is possible to obtain the best ratio of structural weight to gross weight and to ensure the structural integrity of the vehicle.

Shell structures offer excellent weight and fabrication characteristics for use in missile and space structures. It is the purpose of this report to present methods of analysis for several problems encountered in this type of structure. The membrane stresses produced by the pressurization of such shells are usually easily computed. However, the forces and stresses involved in the discontinuity regions are not so readily determined, and the published techniques of solution are in many cases of such a nature as to preclude their use by the design engineer. There are four basic difficulties involved. First, for some problems no solution exists in the published literature. Second, many of the published solutions involve mathematical complexities beyond the background of the average designer. Third, a large proportion of the solutions, as presented, are not carried to the point where they can be used directly for determining stress distributions. Fourth, many of the solutions, depending on the assumptions involved, require calculations of an extensive and tedious nature.

In general, the more rigorous solutions are based on few assumptions and lead to difficult analyses which are of no practical use to the designer. It is necessary to sacrifice some degree of accuracy to obtain a solution in a reasonably direct mathematical manner. The degree of accuracy that is required and the degree of complexity that is considered acceptable are factors which must be weighed in selecting a method of analysis for any shell problem.

An attempt was therefore made in the preparation of this paper to survey the literature to sort out the more practical types of solutions. It was necessary to expand some of the solutions extensively to obtain expresssions for all the internal forces. From these, complete stress distributions and the maximum stresses and their locations were determined. The selected solutions, as modified and extended, are compiled in this report in a form which can be readily used by the average

engineer. These solutions include treatment of the following problems:

(A) Deflection, rotation, and internal stresses in the following edge-loaded shells of revolution:
(1) Right circular cylinder
(2) Frustum of a right circular cone
(3) Portion of a sphere
(B) Discontinuity shear and moment at the following shell junctions:
(1) Axial change of thickness in a circular cylinder
(2) Axial change of thickness in a cone
(3) Change of thickness in a sphere
(4) Junction of a cylinder and a cone
(5) Junction of a cylinder and a portion of a sphere
(6) Junction of a cylinder and a flat head
(7) Junction of a cone and a portion of a sphere

The analyses for the changes in thickness are intended as an investigation of the edge effect of chemically milled or machined surfaces where an abrupt change of thickness symmetrical about the middle surface occurs. Several special cases can be deduced from those just given. The equations for the edge-loaded portion of a sphere can be specialized to give the case of an edge-loaded hemisphere. The solution for the junction of a cylinder and a portion of a sphere will yield the special case of a cylinder with a hemispherical dome. The solution of a cylinder with fixed ends can be obtained from the case of the cylinder with a flat head. The solution of a junction of a cone and a portion of a sphere has the special case in which the cone and spherical shell have a common tangent to their meridians at the junction. This solution combined with the solution for a cylinder with a hemispherical dome will yield the solution of a toriconical head in which the torus is a portion of a sphere.

Only the final equations and parameters necessary for the solution of any of the cases are given in the body of the report. The derivations, together with intermediate equations and some discussion, are presented as appendixes A to L.

SYMBOLS

a radius of cylinder, in.
c thickness ratio
D $Eh^3/12(1-\nu^2)$, lb-in.
E modulus of elasticity, psi
H radial shear force in wall of shell acting on a plane perpendicular to axis of revolution, lb/in.
h thickness of shell wall, in.
M bending moment in wall of shell, in.-lb/in.
m $\sqrt[4]{12(1-\nu^2)}$
N uniform normal force in wall of shell, lb/in.
p internal pressure, lb/sq in.
Q shear force perpendicular to wall of shell, lb/in.
R radius of spherical shell, in.
r radius of parallel circle, in.
V angle of rotation of a tangent to a meridian, radians
$\overline{w}$ deflection perpendicular to axis of revolution, in.
x distance along meridian from edge of cylinder, in.
y distance along meridian from apex of cone, in.
α half-angle of cone or portion of sphere, radians
β $\sqrt[4]{3(1-\nu^2)/a^2h^2}$, in.$^{-1}$
δ edge-deflection influence coefficient
$\Theta(\ )$ $e^{-(\ )}\cos(\ )$
λ $\sqrt[4]{3(1-\nu^2)R^2/h^2}$
μ $\sqrt[4]{12(1-\nu^2)/h^2\tan^2\alpha}$, in.$^{-1/2}$
ν Poisson's ratio
ξ $2\mu\sqrt{y}$
σ normal stress, psi
τ shear stress, psi
$\Phi(\ )$ $e^{-(\ )}[\cos(\ )+\sin(\ )]$
φ angular measure in plane containing meridian and axis of revolution, radians
$\Psi(\ )$ $e^{-(\ )}[\cos(\ )-\sin(\ )]$
$\Omega(\ )$ $e^{-(\ )}\sin(\ )$
ω edge-rotation influence coefficient

Subscripts:
c cylinder
f flat head
i, j dummy indices
k cone
m meridional
s spherical shell
x meridional direction on cylinder
y meridional direction on cone
θ circumferential
τ shear
φ meridional direction on spherical shell
0 junction
1,2 different thicknesses at change of thickness

Because some subscripts are used only once or twice, they are, for purposes of brevity, defined where they occur and not listed here. This is particularly true for many parameters appearing in the cone analyses. Also, the usage of a number of subscripts is considered self-evident, and no amplification of their meaning is given.

METHOD OF ANALYSIS

In the design of pressure vessels, certain regions frequently exist where continuity of the structure cannot be satisfied by membrane forces alone. Such regions are known as "discontinuity" areas. The discontinuity forces which are induced to make the rotations and deflections of the walls continuous are usually of a local nature, but they may considerably alter the stress distributions in the regions where they occur. It is assumed in this report that, where more than one discontinuity is present, the distance between them is sufficient that each does not noticeably affect the discontinuity shear and moment of the other.

All shells are rotationally symmetric and loaded by internal pressure. The stresses due to the weight of the structure are not considered. These are usually much smaller than those due to internal pressure and may frequently be neglected without introducing noticeable error. The stresses due to dead weight, supports, concentrated loads, or other such conditions can be superimposed upon those presented here when such conditions exist and are significant.

The usual method of determining the discontinuity forces is to imagine the shell to be physically separated at the discontinuity. The edges of the two components will, in general, rotate and deflect different amounts if the membrane stresses alone are considered. Deflections and rotations of the edges of the components can be found from conventional membrane analyses. To preserve continuity of rotation and deflection in the actual structure, a discontinuity shear and moment must be present on the edge of each component. Equilibrium of forces at the cross section requires that the shear and moment on the edge of one component be equal and opp site to those on the mating edge of the other component. Having expressions for the edge rotation and deflection of each component due to edge shear and moment, as well as to internal pressure, it is possible to write two equations expressing the equality of deflection and rotation at the discontinuity. These two equations can be solved for the unknown discontinuity shear and moment. Once these have been determined, it is possible to find the rotation, deflection, and internal forces for any element of the shell.

The edge-loaded shells and the regions of the shell on either side of the discontinuity are assumed to have constant thicknesses. The surface described by the revolution of a meridian midway through the thickness is called the middle surface. The middle surface of the shell is assumed to be continuous from one region to another across the discontinuity. Hence, no additional moments are induced by mismatching of the effective lines of action of the meridional forces in the two regions. A discussion and analysis for including the effect of nonconcurrence of the middle surfaces at the junction is presented in appendix L, but it is not used in the body of the report. The shear forces acting on sections made by planes containing the axis of revolution and intersecting the shell are zero because of axial symmetry. Thus the circumferential or hoop stresses acting on these meridional planes (planes containing the axis of revolution and a meridian) are principal stresses.

The normal stresses perpendicular to the middle surface of the shell are neglected, since they are usually much smaller than those in the circumferential and meridional directions. These radial stresses which are neglected vary in magnitude from the value of the pressure on the inside surface of the shell to zero on the outside. Consequently, since the radial stress is neglected, a biaxial stress state is assumed. The direct stresses are assumed uniform throughout the thickness. The bending stresses are assumed to vary linearly through the thickness from zero at the middle surface to maximum values at the inner and outer surfaces.

The shearing stress varies parabolically through the thickness with the maximum occurring at the middle surface and decreases to zero at the inner and outer surfaces. As mentioned before, no shear stresses act on meridional planes. The meridional stresses, that is, stresses acting on planes normal to the meridian, are very nearly equal to principal stresses. This is because the shear stresses are usually much smaller than the normal stresses. In fact, the meridional stresses

on the inner and outer surfaces are principal stresses because the shear stresses are zero at these surfaces.

Because of the nature of the bending stresses, the maximum and minimum stresses will be found on the inner and outer surfaces. When solving for the locations of the maximum stresses, and from these the stresses themselves, the usual theory of maximums and minimums is employed. Since the equations for stress are exponentially decaying sine functions, more than one solution will be found for the possible location. However, only the smallest positive value of the independent variable so obtained is significant.

The maximum stress sometimes occurs at the loaded edge of the shell when the slope of the combined stress curve has a nonzero value. Therefore, when solving for maximum stresses, it is always necessary to check the loaded edge of the shell in addition to the location of zero slope nearest to the loaded edge. Because of the bending stresses, both the inner and outer surfaces must be checked for the maximum stress. By checking both surfaces, both the maximum and minimum stresses will be obtained.

The material is assumed to be homogeneous and isotropic and to obey Hooke's law. The results are applicable only to stresses within the elastic region for thin-walled pressure vessels. Also, small deflections are assumed throughout the report in the derivation of the basic equations.

SUMMARY OF SOLUTIONS

The summaries are arranged here in the order in which they would ordinarily be used. First, the discontinuity shear and moment are determined for the particular shell junction being considered. Having determined these, it is only necessary to substitute them into the corresponding edge-loaded shell equations to determine the stress distributions. The arrangement of the summaries is not the same as the order in which they are derived in the appendixes. This is because some of the equations derived for the edge-loaded shells were necessary for the solution of the junction problems. Consequently, the edge-loaded shell solutions appear first in the appendixes.

DETERMINATION OF DISCONTINUITY SHEAR FORCES AND BENDING MOMENTS

Shear and moment at an axial change of thickness in a circular cylinder.—Referring to figure 1 for sign convention, the discontinuity shear and moment for this case are

$$Q_0=\frac{2-\nu}{2\beta_1}\left[\frac{(c-1)(c^{5/2}+1)}{(c^2+1)^2+2c^{3/2}(c+1)}\right]p \tag{1}$$

and

$$M_0=\frac{2-\nu}{4\beta_1^2}\left[\frac{(c-1)(c^2-1)}{(c^2+1)^2+2c^{3/2}(c+1)}\right]p \tag{2}$$

where

$$c=\frac{h_1}{h_2} \tag{3}$$

and the subscript 1 refers to the cylinder with thickness h_1. Because of the sign convention chosen in figure 1, the sign for Q_0 must be changed when solving for the stresses in the cylinder of thickness h_2.

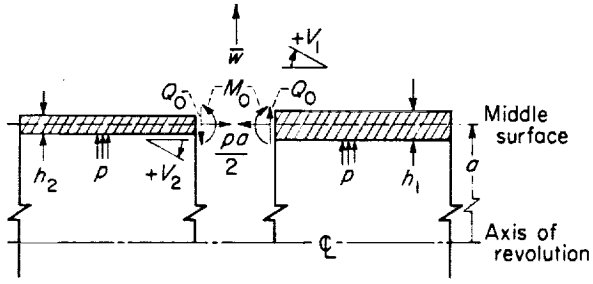

FIGURE 1.—Change of thickness in cylinder.

Shear and moment at an axial change of thickness in a cone.—With the sign convention as shown in figure 2, the discontinuity shear and moment for this case are

$$H_0=\frac{(\delta_{1,M_0}-\delta_{2,M_0})(\omega_{1,p}-\omega_{2,p})-(\delta_{1,p}-\delta_{2,p})(\omega_{1,M_0}-\omega_{2,M_0})}{(\delta_{1,H_0}-\delta_{2,H_0})(\omega_{1,M_0}-\omega_{2,M_0})-(\delta_{1,M}-\delta_{2,M_0})(\omega_{1,H_0}-\omega_{2,H_0})}p \tag{4}$$

and

$$M_0=\frac{(\delta_{1,p}-\delta_{2,p})(\omega_{1,H_0}-\omega_{2,H_0})-(\delta_{1,H_0}-\delta_{2,H_0})(\omega_{1,p}-\omega_{2,p})}{(\delta_{1,H_0}-\delta_{2,H_0})(\omega_{1,M_0}-\omega_{2,M_0})-(\delta_{1,M_0}-\delta_{2,M_0})(\omega_{1,H_0}-\omega_{2,H_0})}p \tag{5}$$

The subscripts 1 and 2 refer to the regions of thicknesses h_1 and h_2, respectively. The expressions for the edge influence coefficients are obtained from their more general counterparts presented in the section "Frustum of a cone loaded by edge shear and moment and internal pressure." For the problem being considered here, $y_1=y_2=y_0$ and $r_1=r_2=r_0$, but λ and ξ are not the same for the two edges at the junction, because h_1 does not equal h_2. Therefore,

$$\left.\begin{aligned} \xi_1&=2\mu_1\sqrt{y_0} \qquad \mu_1=\frac{m}{\sqrt{h_1\tan\alpha}} \\ \xi_2&=2\mu_2\sqrt{y_0} \qquad \mu_2=\frac{m}{\sqrt{h_2\tan\alpha}} \end{aligned}\right\} \tag{6}$$

The parameters λ_1, ξ_1, ω_1, and δ_1 are associated with the region of thickness h_1; likewise, λ_2, ξ_2, ω_2, and δ_2 are associated with h_2.

The expressions for the edge influence coefficient are

$$\left.\begin{aligned}
\omega_{1,M_0}&=-\frac{m^3}{Eh_1^2}\sqrt{\frac{2r_0}{h_1\cos\alpha}}\,\Omega_1 \\
\omega_{1,H_0}&=\frac{m^2r_0}{Eh_1^2}\,\Omega_2 \\
\omega_{1,p}&=\frac{m^2r_0^2\tan\alpha}{2Eh_1^2}\Omega_2+\frac{3(1+\nu)\tan^2\alpha}{mE}\sqrt{\frac{r_0}{2h_1\cos\alpha}}\,\Omega_1-\frac{3r_0\tan\alpha}{2Eh_1\cos\alpha} \\
\delta_{1,M_0}&=\frac{m^2r_0}{Eh_1^2}\,\Omega_2 \\
\delta_{1,H_0}&=-\frac{mr_0}{Eh_1}\sqrt{\frac{2r_0\cos\alpha}{h_1}}\,\Omega_3 \\
\delta_{1,p}&=-\frac{mr_0^2\sin\alpha}{Eh_1}\sqrt{\frac{r_0}{2h_1\cos\alpha}}\,\Omega_3-\frac{m^2r_0\tan^2\alpha}{8(1-\nu)E}\,\Omega_2+\frac{\left(1-\frac{\nu}{2}\right)r_0^2}{Eh_1\cos\alpha} \\
\omega_{2,M_0}&=\frac{m^3}{Eh_2^2}\sqrt{\frac{2r_0}{h_2\cos\alpha}}\,\Omega_4 \\
\omega_{2,H_0}&=\frac{m^2r_0}{Eh_2^2}\,\Omega_5 \\
\omega_{2,p}&=\frac{m^2r_0^2\tan\alpha}{2Eh_2^2}\,\Omega_5-\frac{3(1+\nu)\tan^2\alpha}{mE}\sqrt{\frac{r_0}{2h_2\cos\alpha}}\,\Omega_4-\frac{3r_0\tan\alpha}{2Eh_2\cos\alpha} \\
\delta_{2,M_0}&=\frac{m^2r_0}{Eh_2^2}\,\Omega_5 \\
\delta_{2,H_0}&=\frac{mr_0}{Eh_2}\sqrt{\frac{2r_0\cos\alpha}{h_2}}\,\Omega_6 \\
\delta_{2,p}&=\frac{mr_0^2\sin\alpha}{Eh_2}\sqrt{\frac{r_0}{2h_2\cos\alpha}}\,\Omega_6-\frac{m^2r_0\tan^2\alpha}{8(1-\nu)E}\,\Omega_5+\frac{\left(1-\frac{\nu}{2}\right)r_0^2}{Eh_2\cos\alpha}
\end{aligned}\right\} \tag{7}$$

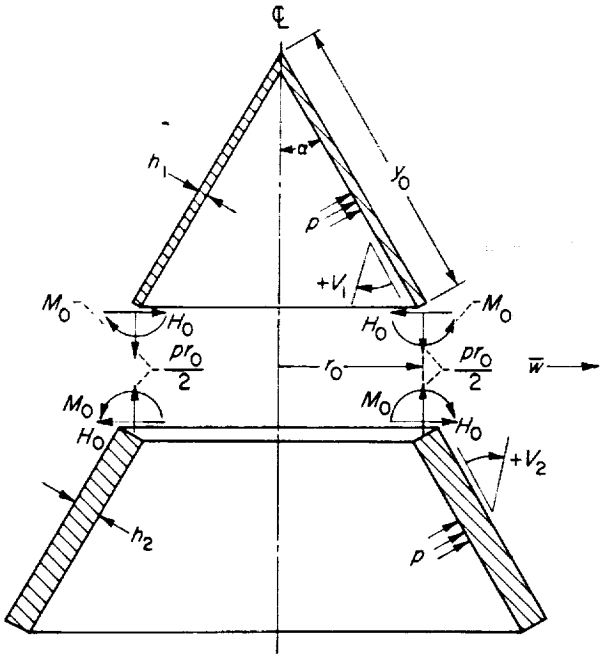

FIGURE 2.—Change of thickness in cone.

where

$$\left.\begin{aligned}
\Omega_1&=\frac{\xi_1 G}{\sqrt{2}(C+2\nu G)} & \Omega_4&=\frac{-\xi_2 G_K}{\sqrt{2}(C_K+2\nu G_K)}\\
\Omega_2&=\frac{-A}{C+2\nu G} & \Omega_5&=\frac{-A_K}{C_K+2\nu G_K}\\
\Omega_3&=\frac{\xi_1 B-\dfrac{4\nu^2 G}{\xi_1}}{\sqrt{2}(C+2\nu G)} & \Omega_6&=\frac{-\xi_2 B_K+\dfrac{4\nu^2 G_K}{\xi_2}}{\sqrt{2}(C_K+2\nu G_K)}
\end{aligned}\right\} \quad (8)$$

and

$$\left.\begin{aligned}
A&=\xi_1(ber'_2\xi_1\ bei_2\xi_1-bei'_2\xi_1\ ber_2\xi_1)\\
B&=(ber'_2\xi_1)^2+(bei'_2\xi_1)^2\\
C&=\xi_1\ (ber_2\xi_1\ ber'_2\xi_1+bei_2\xi_1\ bei'_2\xi_1)\\
G&=(ber_2\xi_1)^2+(bei_2\xi_1)^2\\
A_K&=\xi_2(ker'_2\xi_2\ kei_2\xi_2-kei'_2\xi_2\ ker_2\xi_2)\\
B_K&=(ker'_2\xi_2)^2+(kei'_2\xi_2)^2\\
C_K&=\xi_2\ (ker_2\xi_2\ ker'_2\xi_2+kei_2\xi_2\ kei'_2\xi_2)\\
G_K&=(ker_2\xi_2)^2+(kei_2\xi_2)^2
\end{aligned}\right\} \quad (9)$$

Figure 3, taken from reference 1, can also be used to determine graphically the Ω functions for certain ranges of ξ. If the analytical expressions are

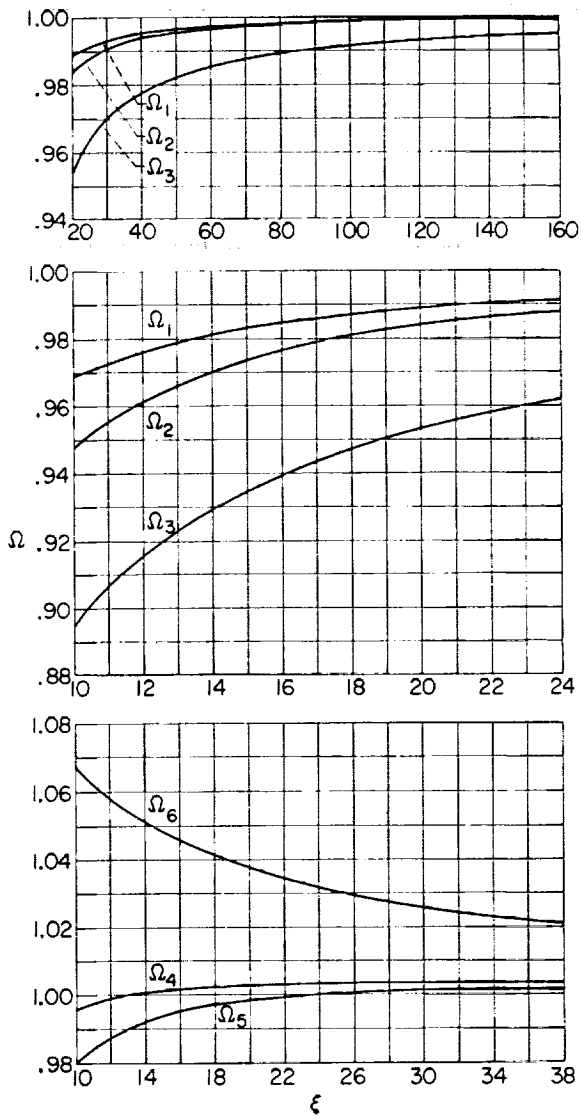

FIGURE 3.—Functions used in analysis of conical shells (based on $\nu=0.3$).

used, reference 2 can be used to find values for the Bessel-Kelvin functions and their derivatives up to arguments of 107.5. For large arguments, the following asymptotic expressions may be used:

$$\left.\begin{aligned}
\Omega_1&\approx 1-\frac{\sqrt{2}}{10\xi}-\frac{1.855}{\xi^2} & \Omega_4&\approx 1+\frac{\sqrt{2}}{10\xi}-\frac{1.855}{\xi^2}\\
\Omega_2&\approx 1-\frac{\sqrt{2}}{10\xi}-\frac{3.730}{\xi^2} & \Omega_5&\approx 1+\frac{\sqrt{2}}{10\xi}-\frac{3.730}{\xi^2}\\
\Omega_3&\approx 1-\frac{0.84853}{\xi}-\frac{1.865}{\xi^2} & \Omega_6&\approx 1+\frac{0.84853}{\xi}-\frac{1.865}{\xi^2}
\end{aligned}\right\} \quad (10)$$

The desired discontinuity shear and moment are now found by use of equations (4) and (5), respectively. Essentially all of the preceding analysis is taken directly from reference 1. The nomenclature is essentially the same as in reference 1 except for some differences due to changes in sign convention.

Shear and moment at a change of thickness in a portion of a sphere.—The discontinuity shear and moment for this case are

$$H_0=\frac{(1-\nu)R}{2\lambda_1 \sin\alpha}\left[\frac{(1-c)(1+c^{5/2})}{(1+c^2)^2+2c^{3/2}(1+c)}\right]p \quad (11)$$

and

$$M_0=\frac{(1-\nu)R^2}{4\lambda_1^2}\left[\frac{(1-c)(1-c^2)}{(1+c^2)^2+2c^{3/2}(1+c)}\right]p \quad (12)$$

where

$$c=\frac{h_1}{h_2} \quad (13)$$

and the sign convention is as shown in figure 4. The subscript 1 refers to the portion of the sphere with thickness h_1. Because of the sign convention used in figure 4, the sign for H_0 must be changed when solving for the stresses in the region of thickness h_2. Also, the angle $(\pi-\alpha)$ must be substituted for α in the stress equations for thickness h_2.

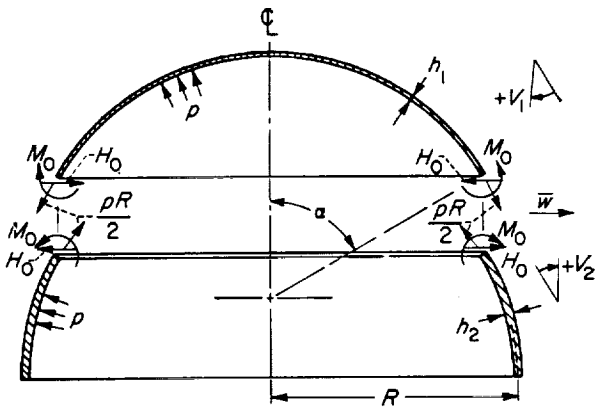

FIGURE 4.—Change of thickness in sphere.

Shear and moment at the junction of a cylinder and a cone.—In this case the discontinuity shear and moment are

$$H_0=\frac{\omega_{k,p}(\delta_{k,M_0}-\delta_{c,M_0})-(\delta_{k,p}-\delta_{c,p})(\omega_{k,M_0}-\omega_{c,M_0})}{(\delta_{k,H_0}-\delta_{c,H_0})(\omega_{k,M_0}-\omega_{c,M_0})-(\delta_{k,M_0}-\delta_{c,M_0})(\omega_{k,H_0}-\omega_{c,H_0})}\,p \quad (14)$$

and

$$M_0=\frac{(\delta_{k,p}-\delta_{c,p})(\omega_{k,H_0}-\omega_{c,H_0})-\omega_{k,p}(\delta_{k,H_0}-\delta_{c,H_0})}{(\delta_{k,H_0}-\delta_{c,H_0})(\omega_{k,M_0}-\omega_{c,M_0})-(\delta_{k,M_0}-\delta_{c,M_0})(\omega_{k,H_0}-\omega_{c,H_0})}\,p \quad (15)$$

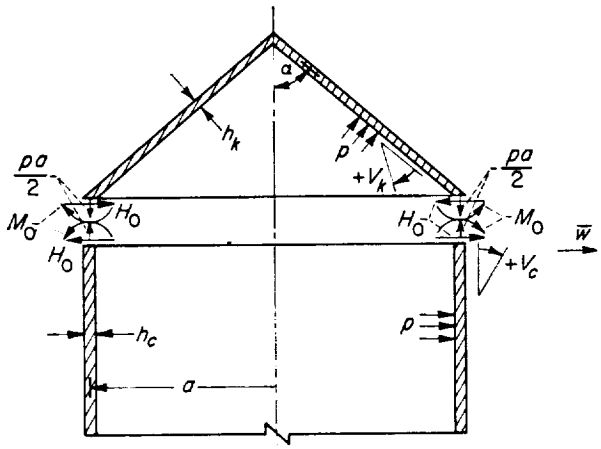

FIGURE 5.—Junction of cone and cylinder.

where the subscripts c and k refer to the cylinder and cone, respectively. Most of the edge influence coefficients appearing in the preceding equations are evaluated from the expressions found in the summaries for the edge-loaded cylinder and edge-loaded cone (eqs. (30) and (38)). In addition, from membrane theory

and

$$\left.\begin{aligned}\omega_{c,p}&=0\\ \delta_{c,p}&=\frac{a^2}{Eh_c}\left(1-\frac{\nu}{2}\right)\end{aligned}\right\} \quad (16)$$

The sign convention for H_0 and M_0 is given in figure 5.

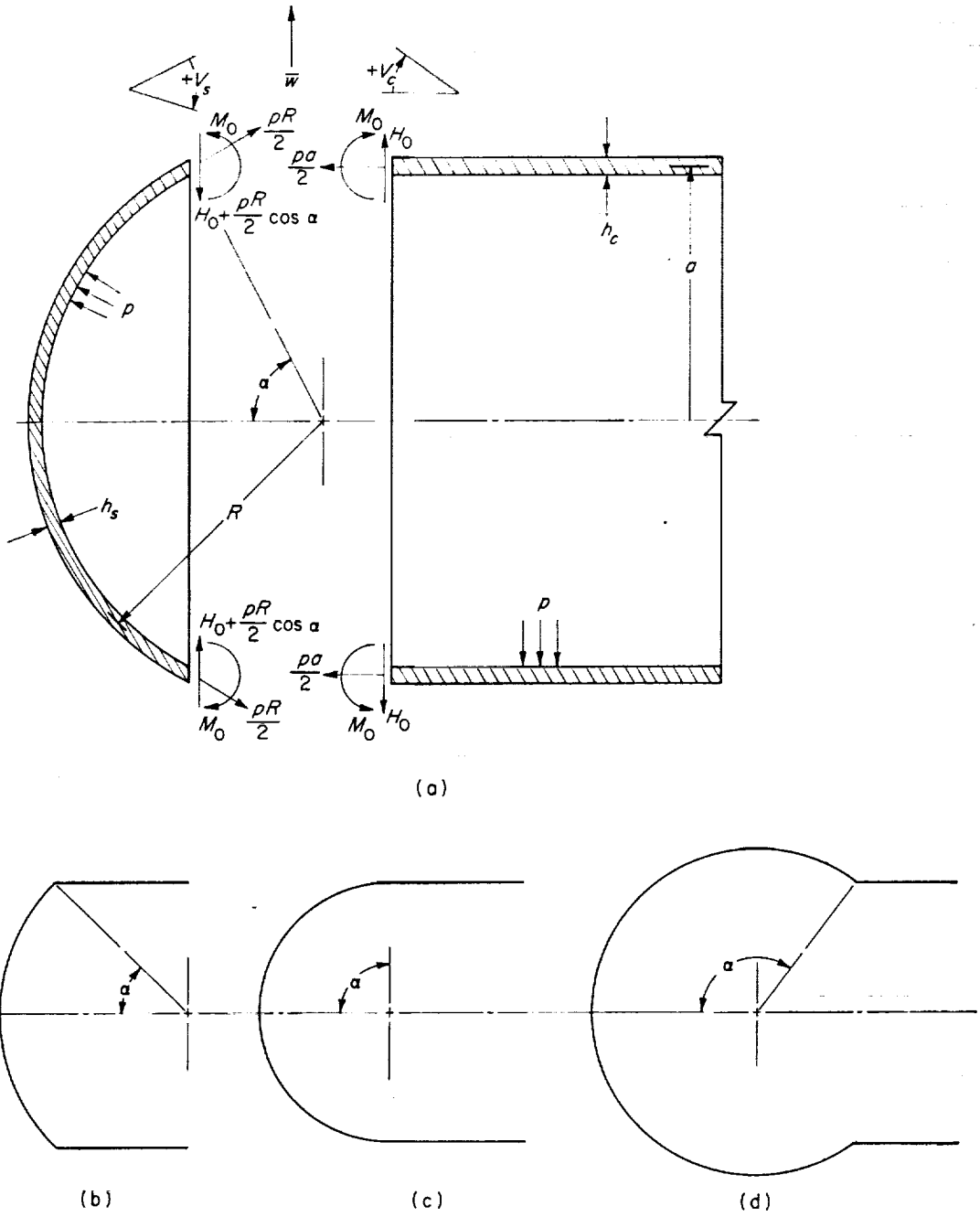

(a) Geometry and sign convention.
(b) $\alpha<90°$.
(c) $\alpha=90°$.
(d) $\alpha>90°$.

FIGURE 6.—Junction of cylinder and portion of sphere.

Shear and moment at the junction of a cylinder and a portion of a sphere.—Referring to figure 6(a) for the sign convention, the discontinuity shear and moment for this shell junction are

$$H_0=\left\{\frac{\left[\frac{1-\nu}{\sin\alpha}-(2-\nu)c\right][1+c^2\sqrt{c\sin\alpha}]\frac{1}{\lambda_s}-[1+c^2+2c^2\sqrt{c\sin\alpha}]\cos\alpha}{(1+c^2)^2+\frac{2c^2}{\sqrt{c\sin\alpha}}(1+c\sin\alpha)}\right\}\frac{pR}{2} \tag{17}$$

and

$$M_0=\left\{\frac{\left[\frac{1-\nu}{\sin\alpha}-(2-\nu)c\right]\left[\frac{1-c^2}{2\lambda_s^2}\right]+\left[\left(1+\frac{1}{\sqrt{c\sin\alpha}}\right)\frac{c^2}{\lambda_s}\right]\cos\alpha}{(1+c^2)^2+\frac{2c^2}{\sqrt{c\sin\alpha}}(1+c\sin\alpha)}\right\}\frac{paR}{2} \tag{18}$$

where the subscript c refers to the cylinder and s to the portion of a sphere and

$$c=\frac{h_s}{h_c} \tag{19}$$

Equations (17) and (18) are true whether α is greater than or less than 90° (see fig. 6). For the particular case $\alpha=90°$, or $R=a$, the solution is obtained for a cylinder with a hemispherical dome. Note that, when solving for the stresses and displacements in the spherical portion of the shell, $H_0+\frac{pR}{2}\cos\alpha$ is substituted for H_0 in equations (42) to (52) (see fig. 6(a)) for this case.

Shear and moment at the junction of a cylinder and a flat head.—The discontinuity shear and moment for this case are

$$H_0=-\left\{\frac{c^3\lambda_c^3+2(2-\nu)c^3\lambda_c+2(2-\nu)(1+\nu)}{2c^3\lambda_c^2+[(1-\nu)c^4+(1+\nu)]\lambda_c+(1-\nu^2)c}\right\}\frac{a}{4}p \tag{20}$$

and

$$M_0=\left\{\frac{2c^3\lambda_c^3+(1-\nu)c^4\lambda_c^2+2(2-\nu)(1+\nu)}{2c^3\lambda_c^2+[(1-\nu)c^4+(1+\nu)]\lambda_c+(1-\nu^2)c}\right\}\frac{a^2}{8\lambda_c}p \tag{21}$$

where

$$c=\frac{h_c}{h_f} \tag{22}$$

and the subscripts c and f refer to the cylinder and flat head, respectively. The sign convention is given in figure 7. If the thickness of the flat plate is very large in comparison with the thickness of the cylinder ($h_f \gg h_c$), c approaches zero and the solution for a cylinder with fixed ends free to expand axially is obtained.

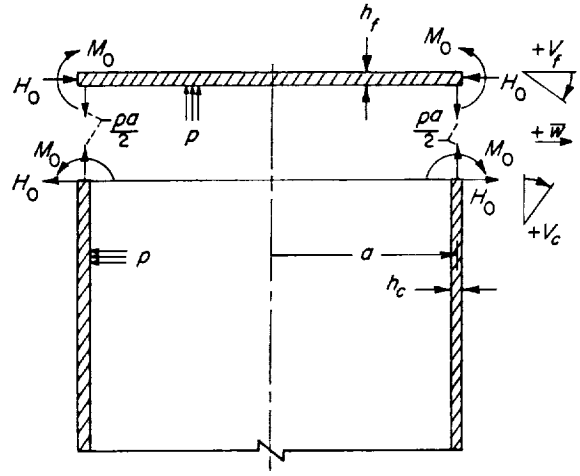

FIGURE 7.—Junction of cylinder and flat head.

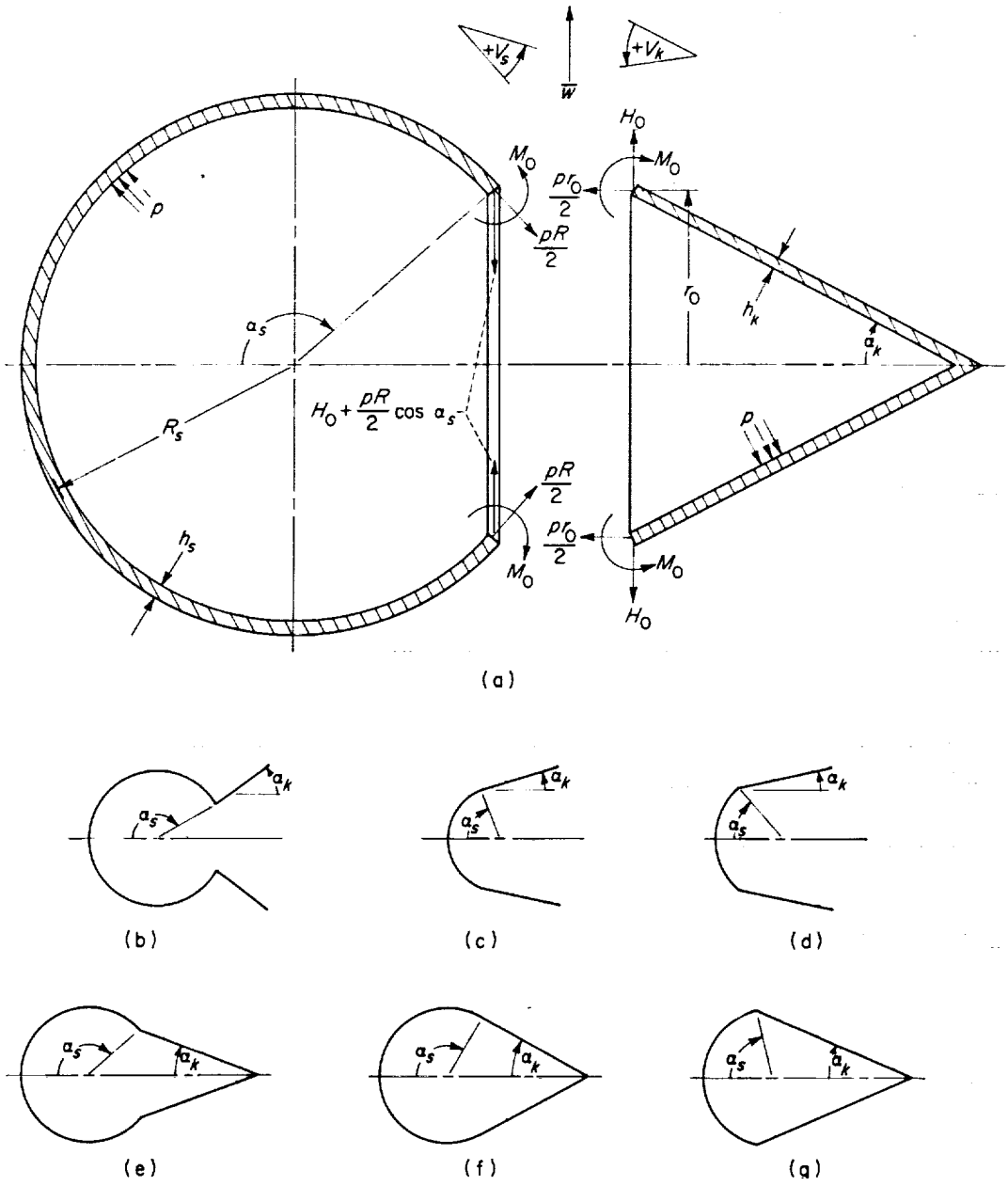

(a) Geometry and sign convention.

(b) $\alpha_s > \frac{\pi}{2} - \alpha_k$. (c) $\alpha_s = \frac{\pi}{2} - \alpha_k$. (d) $\alpha_s < \frac{\pi}{2} - \alpha_k$.

(e) $\alpha_s > \frac{\pi}{2} + \alpha_k$. (f) $\alpha_s = \frac{\pi}{2} + \alpha_k$. (g) $\alpha_s < \frac{\pi}{2} + \alpha_k$.

FIGURE 8.—Junction of cone and portion of sphere.

Shear and moment at the junction of a cone and a portion of a sphere.—Using the sign convention shown in figure 8, the discontinuity shear and moment for this case are

$$H_0=\Big\{\left[\omega_{s,H_0}(\delta_{k,M_0}-\delta_{s,M_0})-\delta_{s,H_0}(\omega_{k,M_0}-\omega_{s,M_0})\right]\frac{R}{2}\cos\alpha_s$$
$$+(\delta_{k,p}-\delta_{s,p})(\omega_{k,M_0}-\omega_{s,M_0})-(\delta_{k,M_0}-\delta_{s,M_0})(\omega_{k,p}-\omega_{s,p})\Big\}p$$
$$\div[(\delta_{k,M_0}-\delta_{s,M_0})(\omega_{k,H_0}-\omega_{s,H_0})-(\delta_{k,H_0}-\delta_{s,H_0})(\omega_{k,M_0}-\omega_{s,M_0})] \tag{23}$$

and

$$M_0=\frac{(\delta_{s,H_0}\omega_{k,H_0}-\delta_{k,H_0}\omega_{s,H_0})\frac{R}{2}\cos\alpha_s+(\delta_{k,H_0}-\delta_{s,H_0})(\omega_{k,p}-\omega_{s,p})-(\delta_{k,p}-\delta_{s,p})(\omega_{k,H_0}-\omega_{s,H_0})}{(\delta_{k,M_0}-\delta_{s,M_0})(\omega_{k,H_0}-\omega_{s,H_0})-(\delta_{k,H_0}-\delta_{s,H_0})(\omega_{k,M_0}-\omega_{s,M_0})}p \tag{24}$$

where the subscripts k and s refer to the cone and the portion of a sphere, respectively. From membrane theory

$$\left.\begin{aligned}&\omega_{s,p}=0\\ \text{and}\quad&\delta_{s,p}=\frac{1-\nu}{2}\frac{R_s^2}{Eh_s}\sin\alpha_s\end{aligned}\right\} \tag{25}$$

The remaining edge influence coefficients are obtained from the summaries for the edge-loaded cone and portion of a sphere (eqs. (38) and (50)) with changes in the signs for ω_{s,H_0} and ω_{s,M_0} due to the change in sign convention for V. Also the signs for ω_{k,H_0} and δ_{k,H_0} must be changed because of the change in sign convention from H_1 to H_0. Because of the sign convention chosen in figure 8, the sign for H_0 must also be changed when it is substituted for H_1 in the equations for the edge-loaded cone to find the stresses (see also fig. 11).

Note that $H_0+\frac{pR}{2}\cos\alpha_s$ is substituted for H_0 in equations (42) to (52) when solving for the stresses and displacements (see fig. 6(a)). The cone and portion of a sphere need not have a common tangent to their meridians at the junction. For the special case where the cone and spherical shell are tangent and the spherical shell is tangent to a cylinder of the same radius, the solution is obtained for a toriconical head that has a torus which is a section of a sphere. The various possible symmetrical junctions of conical frustums and spherical shells are shown in figures 8(b) to (g).

DETERMINATION OF STRESSES AND DEFORMATIONS IN EDGE-LOADED SHELLS

Right circular cylinder loaded by edge shear and moment.—The following equations are applicable at any distance x from the loaded edge of the cylinder. The type and location of stress, as well as the rotation and deflection, are given by equations (26) to (29). Where $\pm$ or $\mp$ signs occur, the upper sign refers to the stresses on the inner surface and the lower sign to the stresses on the outer surface. See figure 9 for the sign convention and figure 10 for curves of the functions Θ, Φ, Ψ, and Ω. Values of these functions are also tabulated in references 3 and 4.

Meridional stress:

$$\sigma_x=\pm\frac{6}{h^2}\left[M_0\Phi(\beta x)+\frac{1}{\beta}Q_0\Omega(\beta x)\right] \tag{26}$$

Circumferential stress:

$$\sigma_\theta=\left[2\beta^2\frac{a}{h}\Psi(\beta x)\pm\frac{6\nu}{h^2}\Phi(\beta x)\right]M_0+\left[2\beta\frac{a}{h}\Theta(\beta x)\pm\frac{6\nu}{\beta h^2}\Omega(\beta x)\right]Q_0 \tag{27}$$

Rotation of meridian:

$$V=\frac{1}{2\beta^2 D}\left[2\beta M_0\Theta(\beta x)+Q_0\Phi(\beta x)\right] \tag{28}$$

Outward displacement:

$$\bar{w}=\frac{1}{2\beta^3 D}\left[\beta M_0\Psi(\beta x)+Q_0\Theta(\beta x)\right] \tag{29}$$

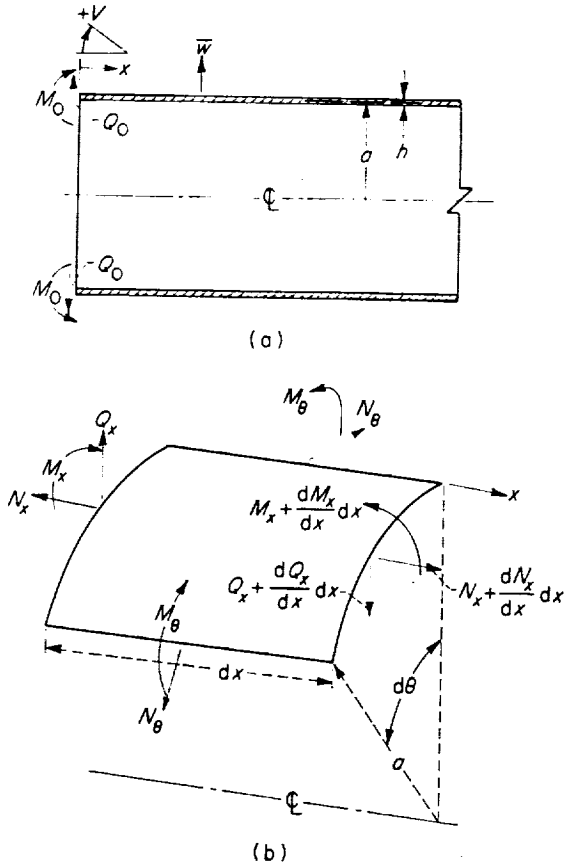

(a) Geometry and loading.
(b) Internal forces and moments.

FIGURE 9.—Cylinder.

At the loaded edge, these equations reduce to

$$(\sigma_x)_{z=0}=\pm\frac{6M_0}{h^2} \tag{26a}$$

$$(\sigma_\theta)_{z=0}=\left(2\beta^2\frac{a}{h}\pm\frac{6\nu}{h^2}\right)M_0+2\beta\frac{a}{h}Q_0 \tag{27a}$$

$$V_0=\frac{1}{2\beta^2D}(2\beta M_0+Q_0)\equiv\omega_{M_0}M_0+\omega_{Q_0}Q_0 \tag{28a}$$

$$\overline{w}_0=\frac{1}{2\beta^3D}(\beta M_0+Q_0)\equiv\delta_{M_0}M_0+\delta_{Q_0}Q_0 \tag{29a}$$

where

$$\left.\begin{aligned}\omega_{M_0}&\equiv\frac{1}{\beta D} & \omega_{Q_0}&\equiv\frac{1}{2\beta^2D}\\ \delta_{M_0}&\equiv\frac{1}{2\beta^2D} & \delta_{Q_0}&\equiv\frac{1}{2\beta^3D}\end{aligned}\right\} \tag{30}$$

The locations of the peak stresses are given by the following equations:
Meridional stress:

$$x_m=\frac{1}{\beta}\arctan\left(\frac{Q_0}{Q_0+2\beta M_0}\right) \tag{31}$$

Circumferential stress:

$$x_\theta=\frac{1}{\beta}\arctan\left[\frac{\mp2\beta m^2M_0+(\mp m^2+6\nu)Q_0}{12\nu\beta M_0+(\pm m^2+6\nu)Q_0}\right] \tag{32}$$

Frustum of a cone loaded by edge shear and moment and internal pressure.—The following equations are applicable at any distance y from the apex of the conical frustum where $y_1\geq y\geq y_2$ (see fig. 11). The type and location of stress, as

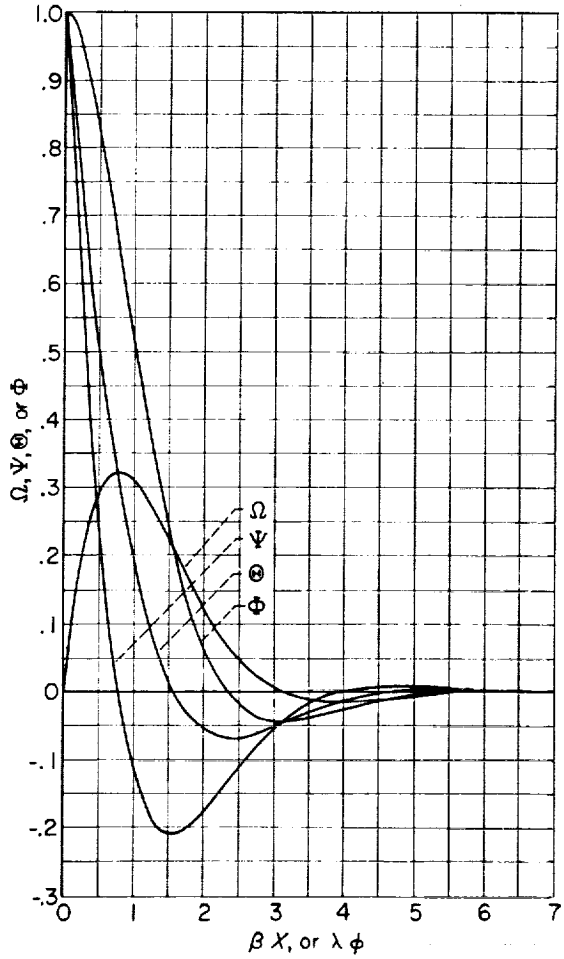

FIGURE 10.—Functions used in analysis of cylindrical and spherical shells.

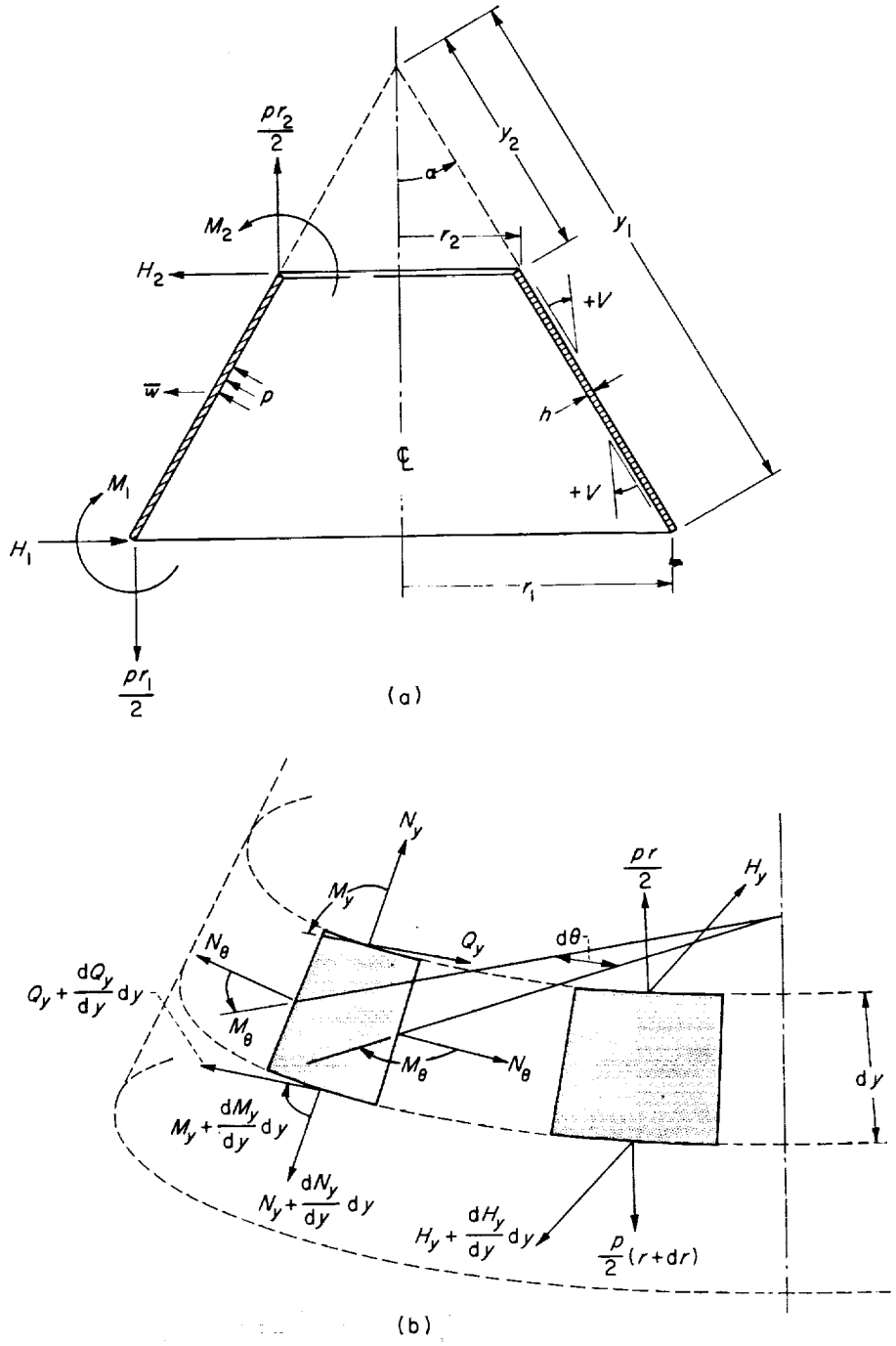

(a) Geometry and loading. (b) Internal forces and moments.

FIGURE 11.—Frustum of cone.

well as the rotation and deflection, are given by equations (33) to (36). Where $\pm$ or $\mp$ signs occur, the upper and lower signs refer to the stresses acting on the inner and outer surfaces, respectively. See figure 11 for the sign convention and loading. The solutions are given in terms of the Bessel-Kelvin functions as tabulated in reference 2. The primes denote differentiation with respect to ξ. Solutions for the constants of integration C_1, C_2, C_3, and C_4, as well as other parameters appearing in the following equations, are given at the end of this summary.

Meridional stress:

$$\sigma_y=\frac{1}{hy}\left\{C_1\left[ber_2\xi\mp\frac{3}{m^2}(\xi bei_2'\xi+2\nu bei_2\xi)\right]\right.$$
$$+C_2\left[bei_2\xi\pm\frac{3}{m^2}(\xi ber_2'\xi+2\nu ber_2\xi)\right]$$
$$+C_3\left[ker_2\xi\mp\frac{3}{m^2}(\xi kei_2'\xi+2\nu kei_2\xi)\right]$$
$$\left.+C_4\left[kei_2\xi\pm\frac{3}{m^2}(\xi ker_2'\xi+2\nu ker_2\xi)\right]\right\}$$
$$+\frac{\tan\alpha}{2}\left(\frac{y}{h}\pm\frac{3}{2}\frac{\tan\alpha}{1-\nu}\right)p \qquad (33)$$

Circumferential stress:

$$\sigma_\theta=\frac{1}{hy}\left\{C_1\left[\frac{\xi}{2}ber_2'\xi\mp\frac{3}{m^2}(2bei_2\xi+\nu\xi bei_2''\xi)\right]\right.$$
$$+C_2\left[\frac{\xi}{2}bei_2''\xi\pm\frac{3}{m^2}(2ber_2\xi+\nu\xi ber_2'\xi)\right]$$
$$+C_3\left[\frac{\xi}{2}ker_2'\xi\mp\frac{3}{m^2}(2kei_2\xi+\nu\xi kei_2''\xi)\right]$$
$$\left.+C_4\left[\frac{\xi}{2}kei_2''\xi\pm\frac{3}{m^2}(2ker_2\xi+\nu\xi ker_2'\xi)\right]\right\}$$
$$+\tan\alpha\left(\frac{y}{h}\pm\frac{3}{4}\frac{\tan\alpha}{1-\nu}\right)p \qquad (34)$$

Rotation of meridian:

$$V=\frac{m^2}{Eh^2}(C_1bei_2\xi-C_2ber_2\xi+C_3kei_2\xi$$
$$-C_4ker_2\xi)-\frac{3}{2}\frac{py\tan^2\alpha}{Eh} \qquad (35)$$

Outward displacement:

$$\overline{w}=\frac{\sin\alpha}{Eh}\left[C_1\left(\frac{\xi}{2}ber_2'\xi-\nu ber_2\xi\right)\right.$$
$$+C_2\left(\frac{\xi}{2}bei_2''\xi-\nu bei_2\xi\right)+C_3\left(\frac{\xi}{2}ker_2'\xi-\nu ker_2\xi\right)$$
$$\left.+C_4\left(\frac{\xi}{2}kei_2''\xi-\nu kei_2\xi\right)\right]+\frac{y^2\sin^2\alpha}{Eh\cos\alpha}\left(1-\frac{\nu}{2}\right)p \qquad (36)$$

These equations reduce to the following equations at the loaded edges, where the subscripts 1 and 2 refer to the edges y_1 and y_2, respectively.

$$\sigma_{y_1}=\frac{y_1\sin\alpha\cos\alpha}{2h}p-\frac{\sin\alpha}{h}H_1\pm\frac{6}{h^2}M_1 \qquad (33a)$$

$$\sigma_{y_2}=\frac{y_2\sin\alpha\cos\alpha}{2h}p-\frac{\sin\alpha}{h}H_2\pm\frac{6M_2}{h^2} \qquad (33b)$$

$$\sigma_{\theta_1}=\frac{3}{4}\frac{\tan^2\alpha}{1-\nu}\left(\frac{\frac{1}{6}m^2A\mp\nu C\mp2G}{C+2\nu G}\pm1\right)p$$
$$+\frac{y_1\tan\alpha}{h}\left(1+\frac{\sin^2\alpha}{2}\frac{\pm6\frac{1-\nu^2}{m^2}A-\frac{\xi_1^2}{2}B-\nu C}{C+2\nu G}\right)p$$
$$+\frac{\sin\alpha}{h}\left(\frac{\pm6\frac{1-\nu^2}{m^2}A-\frac{\xi_1^2}{2}B-\nu C}{C+2\nu G}\right)H_1$$
$$+\frac{6}{h^2}\left(\frac{-\frac{1}{6}m^2A\pm\nu C\pm2G}{C+2\nu G}\right)M_1 \qquad (34a)$$

$$\sigma_{\theta_2}=\frac{3}{4}\frac{\tan^2\alpha}{1-\nu}\left(\frac{1}{6}\frac{m^2A_K\mp\nu C_K\mp2G_K}{C_K+2\nu G_K}\pm1\right)p$$
$$+\frac{y_2\tan\alpha}{h}\left(1+\frac{\sin^2\alpha}{2}\frac{\pm6\frac{1-\nu^2}{m^2}A_K-\frac{\xi_2^2}{2}B_K-\nu C_K}{C_K+2\nu G_K}\right)p$$
$$+\frac{\sin\alpha}{h}\left(\frac{\pm6\frac{1-\nu^2}{m^2}A_K-\frac{\xi_2^2}{2}B_K-\nu C_K}{C_K+2\nu G_K}\right)H_2+\frac{6}{h^2}\left(\frac{-\frac{1}{6}m^2A_K\pm\nu C_K\pm2G_K}{C_K+2\nu G_K}\right)M_2 \qquad (34b)$$

$$V_1=\omega_{1,M_1}M_1+\omega_{1,H_1}H_1+\omega_{1,p}p \qquad (35a)$$

$$V_2=\omega_{2,M_2}M_2+\omega_{2,H_2}H_2+\omega_{2,p}p \qquad (35b)$$

$$\overline{w}_1=\delta_{1,M_1}M_1+\delta_{1,H_1}H_1+\delta_{1,p}p \qquad (36a)$$

$$\overline{w}_2=\delta_{2,M_2}M_2+\delta_{2,H_2}H_2+\delta_{2,p}p \qquad (36b)$$

where

$$C_1=-\frac{\left(H_1y_1h\sin\alpha+\frac{1}{2}phy_1^2\sin^2\alpha\tan\alpha\right)(\xi_1\,ber'_2\xi_1+2\nu\,ber_2\xi_1)+2m^2y_1\,bei_2\xi_1\left[M_1-\frac{ph^2\tan^2\alpha}{8(1-\nu)}\right]}{h(C+2\nu G)} \tag{37a}$$

$$C_2=-\frac{\left(H_1y_1h\sin\alpha+\frac{1}{2}phy_1^2\sin^2\alpha\tan\alpha\right)(\xi_1\,bei'_2\xi_1+2\nu\,bei_2\xi_1)-2m^2y_1\,ber_2\xi_1\left[M_1-\frac{ph^2\tan^2\alpha}{8(1-\nu)}\right]}{h(C+2\nu G)} \tag{37b}$$

$$C_3=-\frac{\left(H_2y_2h\sin\alpha+\frac{1}{2}phy_2^2\sin^2\alpha\tan\alpha\right)(\xi_2\,ker'_2\xi_2+2\nu\,ker_2\xi_2)+2m^2y_2\,kei_2\xi_2\left[M_2-\frac{ph^2\tan^2\alpha}{8(1-\nu)}\right]}{h(C_K+2\nu G_K)} \tag{37c}$$

$$C_4=-\frac{\left(H_2y_2h\sin\alpha+\frac{1}{2}phy_2^2\sin^2\alpha\tan\alpha\right)(\xi_2\,kei'_2\xi_2+2\nu\,kei_2\xi_2)-2m^2y_2\,ker_2\xi_2\left[M_2-\frac{ph^2\tan^2\alpha}{8(1-\nu)}\right]}{h(C_K+2\nu G_K)} \tag{37d}$$

and

$$\left.\begin{aligned}
&\omega_{1,M_1}=-\frac{m^3}{Eh^2}\sqrt{\frac{2r_1}{h\cos\alpha}}\,\Omega_1\\
&\omega_{1,H_1}=\frac{m^2r_1}{Eh^2}\,\Omega_2\\
&\omega_{1,p}=\frac{m^2r_1^2\tan\alpha}{2Eh^2}\,\Omega_2+\frac{3(1+\nu)\tan^2\alpha}{mE}\sqrt{\frac{r_1}{2h\cos\alpha}}\,\Omega_1-\frac{3r_1\tan\alpha}{2Eh\cos\alpha}\\
&\delta_{1,M_1}=\frac{m^2r_1}{Eh^2}\,\Omega_2\\
&\delta_{1,H_1}=-\frac{mr_1}{Eh}\sqrt{\frac{2r_1\cos\alpha}{h}}\,\Omega_3\\
&\delta_{1,p}=-\frac{mr_1^2\sin\alpha}{Eh}\sqrt{\frac{r_1}{2h\cos\alpha}}\,\Omega_3-\frac{m^2r_1\tan^2\alpha}{8(1-\nu)E}\,\Omega_2+\frac{\left(1-\frac{\nu}{2}\right)r_1^2}{Eh\cos\alpha}\\
&\omega_{2,M_2}=\frac{m^3}{Eh^2}\sqrt{\frac{2r_2}{h\cos\alpha}}\,\Omega_4\\
&\omega_{2,H_2}=\frac{m^2r_2}{Eh^2}\,\Omega_5\\
&\omega_{2,p}=\frac{m^2r_2^2\tan\alpha}{2Eh^2}\,\Omega_5-\frac{3(1+\nu)\tan^2\alpha}{mE}\sqrt{\frac{r_2}{2h\cos\alpha}}\,\Omega_4-\frac{3r_2\tan\alpha}{2Eh\cos\alpha}\\
&\delta_{2,M_2}=\frac{m^2r_2}{Eh^2}\,\Omega_5\\
&\delta_{2,H_2}=\frac{mr_2}{Eh}\sqrt{\frac{2r_2\cos\alpha}{h}}\,\Omega_6\\
&\delta_{2,p}=\frac{mr_2^2\sin\alpha}{Eh}\sqrt{\frac{r_2}{2h\cos\alpha}}\,\Omega_6-\frac{m^2r_2\tan^2\alpha}{8(1-\nu)E}\,\Omega_5+\frac{\left(1-\frac{\nu}{2}\right)r_2^2}{Eh\cos\alpha}
\end{aligned}\right\} \tag{38}$$

The remaining parameters necessary for the solution of the cone are given in equations (8) and (9). Equation (10) can also be used where appropriate. As previously mentioned, the cone analysis was taken directly from reference 1.

When H_1, M_1, H_2, and M_2 are set equal to zero, it will be seen that the resulting equations for stress are not the membrane stresses. This is true because the edge support is not the same as that necessary for the membrane condition when there are no edge shears or moments. This must be borne in mind if one wishes to separate the bending stresses from the total stresses at any given point.

The locations of the stress peaks were not determined for this case because of the complicated nature of the stress equations.

Portion of a sphere loaded by edge shear and moment.—The following equations are applicable at any angle φ from the loaded edge of the spherical shell. The type and location of stress, as well as the rotation and deflection, are given by equations (42) to (45). Where $\pm$ or $\mp$ signs occur, the upper sign refers to the stresses on the inner surface and the lower sign to the stresses on the outer surface. See figure 12 for the sign convention and figure 10 for curves of the functions Θ, Φ, Ψ, and Ω. Values of these functions are also tabulated in references 3 and 4.

Meridional stress:

$$\sigma_\varphi=-\left[\frac{2\lambda}{Rh}\cot(\alpha-\varphi)\Omega(\lambda\varphi)\mp\frac{6}{h^2}\Phi(\lambda\varphi)\right]M_0 -\left[\frac{1}{h}\cot(\alpha-\varphi)\Psi(\lambda\varphi)\pm\frac{6R}{\lambda h^2}\Omega(\lambda\varphi)\right]H_0\sin\alpha \tag{42}$$

Circumferential stress:

$$\sigma_\theta=\left[\frac{2\lambda^2}{Rh}\Psi(\lambda\varphi)\pm\frac{6\nu}{h^2}\Phi(\lambda\varphi)\right]M_0 -\left[\frac{2\lambda}{h}\Theta(\lambda\varphi)\pm\frac{6\nu R}{\lambda h^2}\Omega(\lambda\varphi)\right]H_0\sin\alpha \tag{43}$$

Rotation of meridian:

$$V=\frac{2\lambda^2}{Eh}\left[-\frac{2\lambda}{R}\Theta(\lambda\varphi)M_0+\Phi(\lambda\varphi)H_0\sin\alpha\right] \tag{44}$$

Outward displacement:

$$\overline{w}=\frac{2\lambda}{Eh}\sin(\alpha-\varphi)[\lambda\Psi(\lambda\varphi)M_0-R\Theta(\lambda\varphi)H_0\sin\alpha] \tag{45}$$

At the loaded edge, the previous equations reduce to

$$(\sigma_\phi)_{\phi=0}=\pm\frac{6M_0}{h^2}-\frac{H_0\cos\alpha}{h} \tag{46}$$

$$(\sigma_\theta)_{\phi=0}=\left(\frac{2\lambda^2}{Rh}\pm\frac{6\nu}{h^2}\right)M_0-\frac{2\lambda}{h}H_0\sin\alpha \tag{47}$$

$$V_0=\frac{2\lambda^2}{Eh}\left(-\frac{2\lambda}{R}M_0+H_0\sin\alpha\right)\equiv\omega_{M_0}M_0+\omega_{H_0}H_0 \tag{48}$$

$$\overline{w}_0=\frac{2\lambda}{Eh}\sin\alpha\,(\lambda M_0-RH_0\sin\alpha)\equiv\delta_{M_0}M_0+\delta_{H_0}H_0 \tag{4 }$$

where

$$\left.\begin{aligned}\omega_{M_0}&=-\frac{4\lambda^3}{REh} & \omega_{H_0}&=\frac{2\lambda^2\sin\alpha}{Eh}\\ \delta_{M_0}&=\frac{2\lambda^2\sin\alpha}{Eh} & \delta_{H_0}&=-\frac{2\lambda R\sin^2\alpha}{Eh}\end{aligned}\right\} \tag{50}$$

The locations of the peak stresses are given by the following equations:

Meridional stress:

$$\varphi_m=\frac{1}{\lambda}\arctan\left\{\frac{\left[\csc^2(\alpha-\varphi_m)-2\lambda\cot(\alpha-\varphi_m)\pm6\frac{R}{h}\right]RH_0\sin\alpha+2\lambda^2\cot(\alpha-\varphi_m)M_0}{\left[\csc^2(\alpha-\varphi_m)\pm6\frac{R}{h}\right]RH_0\sin\alpha-2\lambda\left[\csc^2(\alpha-\varphi_m)-\lambda\cot(\alpha-\varphi_m)\pm6\frac{R}{h}\right]M_0}\right\} \tag{51}$$

Circumferential stress:

$$\varphi_\theta=\frac{1}{\lambda}\arctan\frac{\left(3\nu\frac{R}{h}\mp\lambda^2\right)RH_0\sin\alpha\pm2\lambda^3M_0}{\left(3\nu\frac{R}{h}\pm\lambda^2\right)RH_0\sin\alpha-6\nu\lambda\frac{R}{h}M_0} \tag{52}$$

It is apparent that equation (51) is transcendental and must be solved by an iterative procedure. Because of this fact and the length of the equation, it might be more advantageous to plot the meridional stress distribution for a short distance using

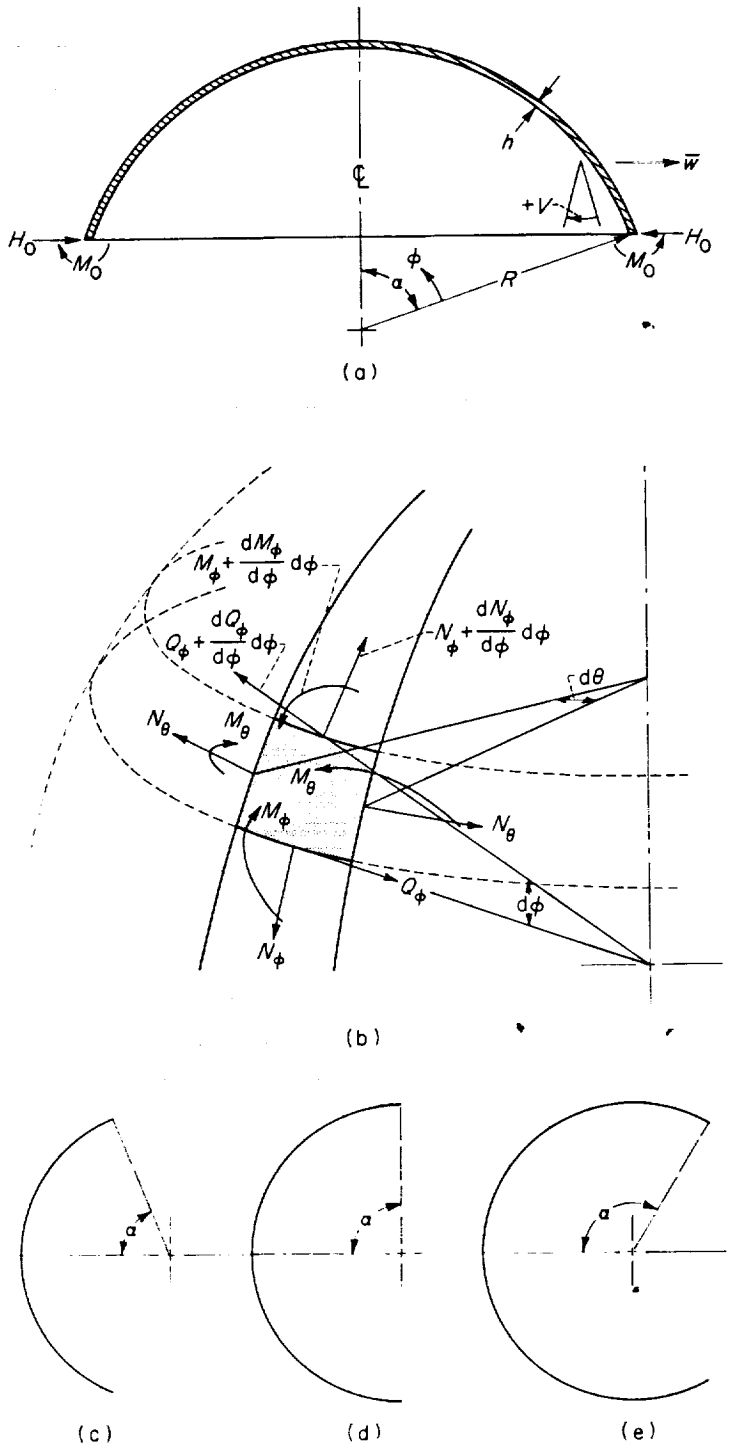

(a) Geometry and loading.
(b) Internal forces and moments.
(c) $\alpha < 90°$.
(d) $\alpha = 90°$.
(e) $\alpha > 90°$.

FIGURE 12.—Portion of sphere.

equation (42). Then the location of the maximum stress, as well as its magnitude and the stress distribution curve, is obtained.

The solution for the edge-loaded hemisphere can be obtained by simply substituting $\alpha=\pi/2$ in the previous equations.

A discussion of edge influence coefficients for thin spherical shells is presented in reference 5. Three different approximate solutions, including the Geckeler approximation used in this section, are obtained for the differential equation of the thin spherical shell. The accuracy of these solutions and recommendations for their use are discussed.

Simply supported circular flat plate with uniform load, edge moment, and edge normal load.—Refer to figure 7 for the geometry, loading, and sign convention for this case. The maximum and minimum stresses are found on the inner and outer surfaces at the center of the plate and are given by

$$(\sigma_r)_{r=0}=(\sigma_\theta)_{r=0}=-\frac{H_0}{h}\pm\frac{6M_0}{h^2}\mp\frac{3(3+\nu)a^2}{8h^2}p \quad (53)$$

where the upper and lower signs refer to the stresses acting on the inner and outer surfaces, respectively. The rotation of the edge of the plate is given by

$$V=-\frac{a}{(1+\nu)D}M_0+\frac{a^3}{8(1+\nu)D}p\equiv\omega_{M_0}M_0+\omega_p p \quad (54)$$

The radial deflection of the edge of the plate is

$$\overline{w}=-\frac{(1-\nu)a}{Eh}H_0\equiv\delta_{H_0}H_0 \quad (55)$$

Given or implied in equations (54) and (55) (see appendix D) is

$$\left.\begin{aligned} \omega_{M_0}&=-\frac{a}{(1+\nu)D} & \delta_{M_0}&=0 \\ \omega_{H_0}&=0 & \delta_{H_0}&=-\frac{(1-\nu)a}{Eh} \\ \omega_p&=\frac{a^3}{8(1+\nu)D} & \delta_p&=0 \end{aligned}\right\} \quad (56)$$

DISCUSSION

In all shell junctions analyzed in this report, the shell is assumed to be long enough that one edge or junction can be analyzed independently of any other. In general, it is not necessary to make this assumption in order to solve for the induced forces at the junctions or for the stresses within a given shell. If the theory is available or can be derived for a given shell, it is only necessary to add two additional simultaneous equations for each junction to account for the close proximity of one junction to another. Then all equations for the junctions that are near each other are solved simultaneously. However, for most shells generally used in engineering practice, the junctions are usually far enough apart to consider each one individually. Thus no serious limitation is incurred by considering each junction separately as is done in this report. The work is considerably simplified because the mathematical difficulty increases very rapidly with the number of simultaneous equations.

The solution for the right circular cylinder is based on theory given in reference 3, as is that for the portion of a sphere. The analysis of the portion of a sphere is not valid in the region of the poles. For edge-loaded spherical segments with small included angles, shallow-shell theory such as in references 5 and 6 should be used.

The analysis chosen for the cone (ref. 1) is essentially an "exact" analysis for relatively long cones, that is, those in which the edge effects do not overlap each other. In reference 7, by use of essentially the same basic differential equations, a solution is obtained for the short conical frustum with edge loads. The equations for both solutions are in terms of Bessel-Kelvin functions. Although it is not possible to present the results for the cone in as concise a form as some of the other shell solutions, most of the work has already been performed in putting them into their present form.

LEWIS RESEARCH CENTER
NATIONAL AERONAUTICS AND SPACE ADMINISTRATION
CLEVELAND, OHIO, *January 5, 1961*

APPENDIX A

RIGHT CIRCULAR CYLINDER LOADED BY EDGE SHEAR AND MOMENT

Consider a thin right circular cylindrical shell, subjected to axially symmetric shear forces and bending moments uniformly distributed along one edge, as in figure 9(a). Because of this loading, the internal forces and moments shown in figure 9(b) arise. According to reference 3 (pp. 466 to 471), the internal forces and moments are given by

$$N_x=0$$

$$N_\theta=2a\beta[\beta M_0\Psi(\beta x)+Q_0\Theta(\beta x)]$$

$$M_x=M_0\Phi(\beta x)+\frac{1}{\beta}Q_0\Omega(\beta x)$$

$$M_\theta=\nu M_x=\nu M_0\Phi(\beta x)+\frac{\nu}{\beta}Q_0\Omega(\beta x)$$

$$Q_x=-2\beta M_0\Omega(\beta x)+Q_0\Psi(\beta x)$$

The equations for the rotation V and the deflection $\overline{w}$ are given as equations (28) and (29) in the text. The functions Θ, Φ, Ψ, and Ω are shown graphically in figure 10. They are also tabulated in references 3 and 4. The largest stresses at a given section corresponding to these forces and moments are

$$\left.\begin{aligned}
\sigma_{N_\theta}&=\frac{N_\theta}{h}=2\beta\frac{a}{h}\left[\beta M_0\Psi(\beta x)+Q_0\Theta(\beta x)\right]\\
\sigma_{M_x}&=\frac{6M_x}{h^2}=\frac{6}{h^2}\left[M_0\Phi(\beta x)+\frac{1}{\beta}Q_0\Omega(\beta x)\right]\\
\sigma_{M_\theta}&=\nu\sigma_{M_x}=\frac{6\nu}{h^2}\left[M_0\Phi(\beta x)+\frac{1}{\beta}Q_0\Omega(\beta x)\right]\\
\tau_x&=\frac{3}{2}\frac{Q_x}{h}=\frac{3}{2h}\left[Q_0\Psi(\beta x)-2\beta M_0\Omega(\beta x)\right]
\end{aligned}\right\}\qquad(A1)$$

The combined stresses in the axial and circumferential directions are

$$\sigma_x=\pm\sigma_{M_x}\qquad(A2)$$

and

$$\sigma_\theta=\sigma_{N_\theta}\pm\sigma_{M_\theta}\qquad(A3)$$

respectively, and, with proper substitution, can be written as equations (26) and (27) in the text. In all instances where $\pm$ or $\mp$ signs occur, the upper sign refers to the inner surface and the lower sign to the outer surface.

Equations (26), (27), and (A1) give the stress distribution throughout the cylinder. In addition to the stress distribution, the locations and magnitudes of the various maximum stresses are usually of considerable interest to the designer. The locations where the various combined stresses are a maximum (except the possibility at the loaded edge) may be obtained by the usual theory of maximums and minimums (see the section METHOD OF ANALYSIS). Equating the derivative of τ_x with respect to x to zero gives

$$x_\tau=\frac{1}{\beta}\arctan\left(1+\frac{Q_0}{\beta M_0}\right)\qquad(A4)$$

where x_τ is the distance from the loaded end of the cylinder to the location of the shear-stress peak. Similarly, the locations of the meridional and circumferential stress peaks are obtained and given as equations (31) and (32) in the text.

APPENDIX B

FRUSTUM OF A CONE LOADED BY EDGE SHEAR AND MOMENT AND INTERNAL PRESSURE

The equations for the internal forces in a conical frustum subjected to edge shears and moments and internal pressure as shown in figure 11(a) can be obtained from references 1 and 8. These are given in terms of the Bessel-Kelvin functions as tabulated in reference 2. With the sign convention as shown in figure 11(b), they are

$$Q_y=\frac{\cot\alpha}{y}\,(C_1\,ber_2\,\xi+C_2\,bei_2\xi+C_3\,ker_2\xi+C_4\,kei_2\xi) \quad \text{(B1a)}$$

$$H_y=\frac{\csc\alpha}{y}\,(C_1\,ber_2\xi+C_2\,bei_2\xi+C_3\,ker_2\xi+C_4\,kei_2\xi)+\frac{py\sin^2\alpha}{2\cos\alpha} \quad \text{(B1b)}$$

$$N_y=\frac{1}{y}\,(C_1\,ber_2\xi+C_2\,bei_2\xi+C_3\,ker_2\xi+C_4\,kei_2\xi)+\frac{py\tan\alpha}{2} \quad \text{(B1c)}$$

$$N_\theta=\frac{\xi}{2y}\,(C_1\,ber_2'\xi+C_2\,bei_2'\xi+C_3\,ker_2'\xi+C_4\,kei_2'\xi)+py\tan\alpha \quad \text{(B1d)}$$

$$M_y=-\frac{h}{2m^2y}\,[C_1(\xi\,bei_2'\xi+2\nu\,bei_2\xi)-C_2(\xi\,ber_2'\xi+2\nu\,ber_2\xi)+C_3(\xi\,kei_2'\xi+2\nu\,kei_2\xi)-C_4(\xi\,ker_2'\xi+2\nu\,ker_2\xi)]+\frac{ph^2\tan^2\alpha}{8(1-\nu)} \quad \text{(B1e)}$$

$$M_\theta=-\frac{h}{2m^2y}\,[C_1(2\,bei_2\xi+\nu\xi\,bei_2'\xi)-C_2(2\,ber_2\xi+\nu\xi\,ber_2'\xi)+C_3(2\,kei_2\xi+\nu\xi\,kei_2'\xi)-C_4(2\,ker_2\xi+\nu\xi\,ker_2'\xi)]+\frac{ph^2\tan^2\alpha}{8(1-\nu)} \quad \text{(B1f)}$$

where

$$\left.\begin{aligned}\xi&=2\mu\sqrt{y}\\ m^4&=12(1-\nu^2)\\ \mu^2&=\frac{m^2}{h\tan\alpha}\end{aligned}\right\} \quad \text{(B2)}$$

and the primes denote differentiation with respect to ξ. The equations for the rotation V and the deflection $\bar{w}$ are given as equations (35) and (36) in the text. The expressions for the constants of integration C_1, C_2, C_3, and C_4 are presented in the text as equations (37) for the loading condition shown in figure 11(a).

The four constants of integration are determined from the following boundary conditions:

$$\left.\begin{aligned}&\text{at } \xi=\xi_1=2\mu\sqrt{y_1} && H_y=-H_1 \quad M_y=M_1\\ &\text{at } \xi=\xi_2=2\mu\sqrt{y_2} && H_y=-H_2 \quad M_y=M_2\end{aligned}\right\} \quad \text{(B3)}$$

As discussed in reference 3 (p. 563), the loads applied at one edge do not appreciably affect the stresses and deformations at the other edge if the cone is sufficiently long. It will be assumed that the thin shells considered here are long enough to conform to the above assumption. This is almost universally true for the conical frustums used in missile and spacecraft applications.

The *ber* and *bei* functions and their derivatives increase rapidly in an oscillatory manner as the distance y increases. Conversely, the *ker* and *kei* functions and their derivatives which also have an oscillatory character decrease rapidly as the distance y increases. Hence, the terms involving *ker* and *kei* and their derivatives are neglected when working near the large end of a conical frustum (or with a complete cone). The constants C_1 and C_2 (which are associated with the *ber* and *bei* functions and their derivatives) are then determined from the boundary conditions at the edge $y=y_1$. Only when working with a frustum of a conical shell are all four constants of integration necessary. The constants C_3 and C_4 (associated with the *ker* and *kei* functions and their derivatives) are determined from the boundary conditions imposed upon the small opening of the truncated cone.

For a long thin-walled conical shell whose half-angle α is not close to $\pi/2$, the calculations can

be simplified by solving two sets of two simultaneous equations instead of one set of four equations. C_3 and C_4 are neglected when evaluating C_1 and C_2 from the conditions at the large end of the frustum, and C_1 and C_2 are neglected when evaluating C_3 and C_4 from the conditions at the small end.

Substituting the boundary conditions at $y=y_1$ into equations (B1b) and (B1e) and neglecting the terms containing C_3 and C_4, the following equations are obtained:

$$-H_1=\frac{\csc\alpha}{y_1}(C_1\, ber_2\xi_1+C_2\, bei_2\xi_1)+\frac{py_1\sin^2\alpha}{2\cos\alpha}$$

$$M_1=-\frac{h}{2m^2y_1}[C_1(\xi_1\, bei_2'\xi_1+2\nu\, bei_2\xi_1)-C_2(\xi_1\, ber_2'\xi_1+2\nu\, ber_2\xi_1)]+\frac{ph^2\tan^2\alpha}{8(1-\nu)}$$

C_1 and C_2 are obtained from these equations and given as equations (37a) and (37b) in the text. Substituting the boundary conditions at $y=y_2$ into equations (B1b) and (B1e) and neglecting the terms containing C_1 and C_2 yield the following two equations:

$$-H_2=\frac{\csc\alpha}{y_2}(C_3\, ker_2\xi_2+C_4\, kei_2\xi_2)+\frac{py_2\sin^2\alpha}{2\cos\alpha}$$

$$M_2=\frac{-h}{2m^2y_2}[C_3(\xi_2\, kei_2'\xi_2+2\nu\, kei_2\xi_2)-C_4(\xi_2\, ker_2'\xi_2+2\nu\, ker_2\xi_2)]+\frac{ph^2\tan^2\alpha}{8(1-\nu)}$$

From these equations, C_3 and C_4 are found and presented as equations (37c) and (37d) in the text.

The closed-form solutions for the four constants of integration can now be substituted into equations (B1) to determine the complete distribution of internal forces. As was true in the derivation of the constants, the terms containing C_3 and C_4 can be neglected when working near the large end of a long frustum (or on a complete cone), and the terms containing C_1 and C_2 can be neglected when working near the small end of a frustum of a long thin-walled conical shell.

The influence coefficients for the edge rotation and deflection of a truncated cone can now be found. Substitute the expressions for the constants of integration (eqs. (37)) into equations (35) and (36) and solve for the edge rotations and deflections. The coefficients of the applied loads will be the desired edge influence coefficients, as shown symbolically in equations (35a), (35b), (36a), and (36b).

The relations between edge loading and edge rotation and deflection can be expressed in terms of the edge coefficients as equations (35a), (35b), (36a), and (36b) in the text, where the subscript 1 refers to the edge of the large end ($y=y_1$) and the subscript 2 to the edge of the small end ($y=y_2$). Using the loading condition shown in figure 11(a) and the sign convention of figure 11(b), the expressions are obtained for the edge influence coefficients and given as equations (38) in the text.

The meridional stresses and the circumferential stresses are given by

$$\sigma_y=\frac{N_y}{h}\pm\frac{6M_y}{h^2} \tag{B4}$$

and

$$\sigma_\theta=\frac{N_\theta}{h}\pm\frac{6M_\theta}{h^2} \tag{B5}$$

respectively. With the proper substitutions, these equations become equations (33) and (34) in the text. In all instances where $\pm$ or $\mp$ signs occur, the upper sign refers to the inner surface and the lower sign to the outer surface. At any given section the maximum shear stress acting on a middle surface is given by

$$\tau=\frac{3}{2}\frac{Q_y}{h}=\frac{3\cot\alpha}{2hy}(C_1\, ber_2\xi+C_2\, bei_2\xi+C_3\, ker_2\xi+C_4\, kei_2\xi) \tag{B6}$$

Equations (33), (34), and (B6) give the complete stress distribution throughout the conical frustum.

APPENDIX C

PORTION OF A SPHERE LOADED BY EDGE SHEAR AND MOMENT

A portion of a sphere subjected to rotationally symmetric uniformly distributed edge loading, as in figure 12(a), will have present internal forces and moments shown in figure 12(b). According to reference 3 (pp. 549 to 551), the internal forces and moments are given by the following (with a change in notation for φ):

$$N_\varphi=-\left[\frac{2\lambda}{R}M_0\Omega(\lambda\varphi)+H_0\,(\sin\alpha)\,\Psi(\lambda\varphi)\right]\cot\,(\alpha-\varphi)$$

$$N_\theta=\frac{2\lambda^2}{R}M_0\Psi(\lambda\varphi)-2\lambda H_0\,(\sin\alpha)\Theta(\lambda\varphi)$$

$$M_\varphi=M_0\Phi(\lambda\varphi)-\frac{R}{\lambda}H_0\,(\sin\alpha)\Omega(\lambda\varphi)$$

$$M_\theta=\nu M_\varphi=\nu M_0\Phi(\lambda\varphi)-\frac{\nu R}{\lambda}H_0(\sin\alpha)\Omega(\lambda\varphi)$$

$$Q_\varphi=\frac{2\lambda}{R}M_0\Omega(\lambda\varphi)+H_0\,(\sin\alpha)\Psi(\lambda\varphi)$$

The equations for the rotation V and the deflection $\overline{w}$ are given as equations (44) and (45) in the text. The functions Θ, Φ, Ψ, and Ω may be obtained from figure 10 or the tables in references 3 and 4.

In this analysis, circumferential stresses (subscript θ) refer to the stresses normal to the cross section obtained by cutting the spherical segment with a plane containing the axis of revolution. Meridional stresses (subscript φ) are those acting on the cross section cut by a cone whose apex is at the center of the sphere and whose axis coincides with the axis of revolution of the spherical segment.

The largest stresses at a given section corresponding to the various internal forces and moments are

$$\left.\begin{aligned}
\sigma_{N_\varphi}&=\frac{N_\varphi}{h}=-\frac{\cot\,(\alpha-\varphi)}{h}\left[\frac{2\lambda}{R}M_0\Omega(\lambda\varphi)+H_0\,(\sin\alpha)\Psi(\lambda\varphi)\right]\\
\sigma_{N_\theta}&=\frac{N_\theta}{h}=\frac{2\lambda^2}{Rh}M_0\Psi(\lambda\varphi)-\frac{2\lambda}{h}H_0\,(\sin\alpha)\,\Theta(\lambda\varphi)\\
\sigma_{M_\varphi}&=\frac{6M_\varphi}{h^2}=\frac{6}{h^2}\left[M_0\Phi(\lambda\varphi)-\frac{R}{\lambda}H_0(\sin\alpha)\,\Omega(\lambda\varphi)\right]\\
\sigma_{M_\theta}&=\frac{6M_\theta}{h^2}=\frac{6\nu}{h^2}\left[M_0\Phi(\lambda\varphi)-\frac{R}{\lambda}H_0(\sin\alpha)\,\Omega(\lambda\varphi)\right]\\
\tau_\varphi&=\frac{3Q_\varphi}{2h}=\frac{3\lambda}{Rh}M_0\Omega(\lambda\varphi)+\frac{3}{2h}H_0(\sin\alpha)\,\Psi(\lambda\varphi)
\end{aligned}\right\}\qquad\text{(C1)}$$

The combined stresses in the meridional and circumferential directions are

$$\sigma_\varphi=\sigma_{N_\varphi}\pm\sigma_{M_\varphi}\qquad\text{(C2)}$$

and

$$\sigma_\theta=\sigma_{N_\theta}\pm\sigma_{M_\theta}\qquad\text{(C3)}$$

respectively, and can be written (with proper substitution) as equations (42) and (43) in the text. Where $\pm$ or $\mp$ signs occur, the upper sign refers to the inner surface and the lower sign to the outer surface.

Equations (42), (43), and (C1) present a complete picture of the stress distribution throughout the spherical segment. From these equations, the locations and magnitudes of the various maximum stresses can be obtained as a further aid to the designer. The points where the com-

bined stresses are a maximum (except for the possibility at the loaded edge) may be found by the usual theory of maximums and minimums (see the section METHOD OF ANALYSIS). Setting the derivative of τ_φ with respect to φ equal to zero and solving for φ give

$$\varphi_r=\frac{1}{\lambda}\text{arc tan}\left(1-\frac{R}{\lambda}\frac{H_0 \sin \alpha}{M_0}\right) \qquad \text{(C4)}$$

where φ_r is the angle between a radius at the loaded edge and a radius (in the same meridional plane) at the location of the shear-stress peak. The locations of the meridional and circumferential stress peaks, given as equations (51) and (52) in the text, are obtained in a similar manner.

The equations presented in this appendix apply to a portion of a spherical shell whose half-angle α may be less than or greater than $\pi/2$ but does not approach 0 or π (fig. 12). The reason for this is that shallow-shell theory (refs. 5 and 6) must be used near the poles. The special case of the edge-loaded hemisphere may be obtained by substituting $\alpha=\pi/2$.

APPENDIX D

SIMPLY SUPPORTED CIRCULAR FLAT PLATE WITH UNIFORM LOAD, EDGE MOMENT, AND EDGE NORMAL LOAD

Consider the case of a simply supported circular flat plate under the action of a uniformly distributed normal load p and with a radially symmetric edge normal load H_0 and an edge moment M_0 as shown in figure 7. The plate can most readily be analyzed as three separate problems and then, by superposition, the final results can be obtained.

Consider first the action of H_0 on the plate. This is a case of hydrostatic plane stress:

$$\sigma_r=\sigma_\theta=-\frac{H_0}{h}$$

The radial deflection at the edge is

$$\overline{w}=-\frac{(1-\nu)a}{Eh}H_0\equiv\delta_{H_0}H_0$$

The surface of the plate remains flat, and therefore

$$\omega_{H_0}=0$$

Next analyze the plate under the influence of M_0. The moment at any point in the plate is M_0. Therefore, the stresses at the inner and outer surfaces are

$$\sigma_r=\sigma_\theta=\pm\frac{6M_0}{h^2}$$

For small deflections normal to the plate, the radial deflection is zero and

$$\delta_{M_0}=0$$

From reference 3 (p. 43) it can be shown that the rotation of the edge of the plate due to M_0 is

$$V=-\frac{aM_0}{(1+\nu)D}\equiv\omega_{M_0}M_0$$

Now consider the simply supported plate acted upon by the uniformly distributed load p. From reference 3 (p. 57) the maximum stresses occur at the center of the plate and are shown to be

$$(\sigma_r)_{max}=(\sigma_\theta)_{max}=\mp\frac{3(3+\nu)a^2}{8h^2}p$$

For small deflections normal to the plate, the radial deflection can once again be assumed zero. Therefore,

$$\delta_p=0$$

The angle of rotation of the edge can be shown to be

$$V=\frac{a^3}{8(1+\nu)D}p\equiv\omega_p p$$

By adding the effects of the conditions described previously, the following results are obtained. The maximum and minimum stresses are found on the inner and outer surfaces at the center of the plate and are given by equation (53) in the text. The edge rotation and deflection are given by equations (54) and (55) in the text, respectively.

APPENDIX E

SHEAR AND MOMENT AT AN AXIAL CHANGE OF THICKNESS IN A CIRCULAR CYLINDER

In this appendix and in the following appendixes the discontinuity shear force and bending moment are determined for several specific shell junctions. Because the derivations for the shear force and bending moment at the various junctions are very similar, they are given here in a general way. These equations are then used with the proper subscripts for the shear and moment in most of the following junction problems.

The general equations for the so-called edge rotations and deflections of two shells, i and j, at their junction can be written in terms of internal pressure, discontinuity shear force and moment, and edge influence coefficients as

$$\left.\begin{aligned} \overline{w}_{0,i} &= \delta_{i,H_0}H_0+\delta_{i,M_0}M_0+\delta_{i,p}p \\ V_{0,i} &= \omega_{i,H_0}H_0+\omega_{i,M_0}M_0+\omega_{i,p}p \\ \overline{w}_{0,j} &= \delta_{j,H_0}H_0+\delta_{j,M_0}M_0+\delta_{j,p}p \\ V_{0,j} &= \omega_{j,H_0}H_0+\omega_{j,M_0}M_0+\omega_{j,p}p \end{aligned}\right\} \tag{E1}$$

The equations for continuity of rotation and deflection at the junction are

$$\left.\begin{aligned} V_{0,i} &= V_{0,j} \\ \overline{w}_{0,i} &= \overline{w}_{0,j} \end{aligned}\right\} \tag{E2}$$

By substituting equations (E1) into equations (E2), the unknown discontinuity shear force and moment are found to be

$$H_0=\frac{(\delta_{i,M_0}-\delta_{j,M_0})(\omega_{i,p}-\omega_{j,p})-(\delta_{i,p}-\delta_{j,p})(\omega_{i,M_0}-\omega_{j,M_0})}{(\delta_{i,H_0}-\delta_{j,H_0})(\omega_{i,M_0}-\omega_{j,M_0})-(\delta_{i,M_0}-\delta_{j,M_0})(\omega_{i,H_0}-\omega_{j,H_0})}p \tag{E3}$$

$$M_0=\frac{(\delta_{i,p}-\delta_{j,p})(\omega_{i,H_0}-\omega_{j,H_0})-(\delta_{i,H_0}-\delta_{j,H_0})(\omega_{i,p}-\omega_{j,p})}{(\delta_{i,H_0}-\delta_{j,H_0})(\omega_{i,M_0}-\omega_{j,M_0})-(\delta_{i,M_0}-\delta_{j,M_0})(\omega_{i,H_0}-\omega_{j,H_0})}p \tag{E4}$$

These equations can now be used with the proper subscripts and edge coefficients to determine the discontinuity forces at most of the junctions considered in this report.

The case considered in this appendix is that of a radially symmetric longitudinal change in the wall thickness of a thin-walled circular cylindrical pressure vessel. The radial expansion of a pressurized cylinder with closed ends due to the membrane stresses is

$$\overline{w}_p=\left(1-\frac{\nu}{2}\right)\frac{pa^2}{Eh}\equiv\delta_p p \tag{E5}$$

This equation applies only at a distance from the closed ends where the effects of the closures are negligible. The membrane stresses cause no rotation of the meridians of a cylinder, and therefore

$$\omega_p=0 \tag{E6}$$

The free radial expansion of a cylinder due to internal pressure is inversely proportional to the wall thickness. Consequently, discontinuity forces and moments must be present which will make the displacements and rotations of two adjacent regions of different wall thicknesses identical at their junction.

Assume the discontinuity forces to be directed as shown in figure 1(a). Refer to equations (E3) and (E4); for this case, $H_0 \equiv Q_0$. Letting subscripts 1 and 2 refer to the regions of thicknesses h_1 and h_2, respectively, the expressions for the unknown discontinuity shear and moment are (with $\omega_p=0$)

$$Q_0=\frac{-(\delta_{1,p}-\delta_{2,p})(\omega_{1,M_0}-\omega_{2,M_0})}{(\delta_{1,Q_0}-\delta_{2,Q_0})(\omega_{1,M_0}-\omega_{2,M_0})-(\delta_{1,M_0}-\delta_{2,M_0})(\omega_{1,Q_0}-\omega_{2,Q_0})}p \tag{E7}$$

$$M_0=\frac{(\delta_{1,p}-\delta_{2,p})(\omega_{1,Q_0}-\omega_{2,Q_0})}{(\delta_{1,Q_0}-\delta_{2,Q_0})(\omega_{1,M_0}-\omega_{2,M_0})-(\delta_{1,M_0}-\delta_{2,M_0})(\omega_{1,Q_0}-\omega_{2,Q_0})}p \tag{E8}$$

If the discontinuity shear and moment are directed as shown and the pressure is internal, then the influence coefficients obtained from equations (E5), (E6), and (30) are as follows:

$$\left.\begin{array}{ll}
\delta_{1,p}=\left(1-\frac{\nu}{2}\right)\frac{a^2}{Eh_1} & \delta_{2,p}=\left(1-\frac{\nu}{2}\right)\frac{a^2}{Eh_2} \\
\delta_{1,Q_0}=\frac{1}{2\beta_1^3 D_1} & \delta_{2,Q_0}=-\frac{1}{2\beta_2^3 D_2} \\
\delta_{1,M_0}=\frac{1}{2\beta_1^2 D_1} & \delta_{2,M_0}=\frac{1}{2\beta_2^2 D_2} \\
\omega_{1,p}=0 & \omega_{2,p}=0 \\
\omega_{1,Q_0}=\frac{1}{2\beta_1^2 D_1} & \omega_{2,Q_0}=\frac{1}{2\beta_2^2 D_2} \\
\omega_{1,M_0}=\frac{1}{\beta_1 D_1} & \omega_{2,M_0}=-\frac{1}{\beta_2 D_2}
\end{array}\right\} \qquad \text{(E9)}$$

Substituting the edge influence coefficients as given in equations (E9) into equations (E7) and (E8) results in equations (1) and (2) in the text for Q_0 and M_0. Because of the sign convention chosen in figure 1(a), the sign for Q_0 must be changed when solving for the stresses in the cylinder of thickness h_2.

APPENDIX F

SHEAR AND MOMENT AT AN AXIAL CHANGE OF THICKNESS IN A CONE

The radial expansion of a conical shell due to internal pressure is a function of the thickness; therefore, if the thickness varies along a meridian, discontinuity forces are induced to make the slopes and deflections continuous along the meridian. The discontinuity shear and moment are determined here in terms of the edge influence coefficients and internal pressure for a truncated conical shell with a radially symmetric sudden change of thickness at a distance y_0 from the apex. Positive shear and moment are as shown in figure 2.

Letting the subscripts 1 and 2 refer to the regions of thicknesses h_1 and h_2, respectively, the expressions for the discontinuity shear and moment can be written as equations (4) and (5) in the text by referring to equations (E3) and (E4).

The expressions for the edge influence coefficients for the cone are given in the section "Frustum of a cone loaded by edge shear and moment and internal pressure." For the problem being considered here, $y_1=y_2=y_0$ and $r_1=r_2=r_0$, but λ and ξ are not the same for the two edges at the junction because h_1 does not equal h_2. The parameters λ_1, ξ_1, ω_1, and δ_1 are associated with the region of thickness h_1; likewise, λ_2, ξ_2, ω_2, and δ_2 are associated with h_2. The expressions for the edge influence coefficients necessary for the solution of H_0 and M_0 are given explicitly as equations (7) in the text.

The desired discontinuity shear and moment are found by use of equations (4) and (5), respectively. The deflection, rotation, and internal stresses at any point in the cone can now be determined by use of the equations in the section "Frustum of a cone loaded by edge shear and moment and internal pressure."

APPENDIX G

SHEAR AND MOMENT AT A CHANGE OF THICKNESS IN A PORTION OF A SPHERE

Consider the case where a change of thickness takes place in a thin-walled spherical shell, symmetrical about an axis as shown in figure 4. The radial expansion due to the membrane stresses only is different in the regions of different thicknesses. The shear and moment required to make the slopes and deflections of the two regions coincide at their junction are determined in the following paragraphs.

Let the subscripts 1 and 2 refer to the regions of thicknesses h_1 and h_2, respectively. Then the expressions for the discontinuity shear and moment can be written in the following manner by referring to equations (E3) and (E4):

$$H_0=\frac{-(\delta_{1,p}-\delta_{2,p})(\omega_{1,M_0}-\omega_{2,M_0})}{(\delta_{1,H_0}-\delta_{2,H_0})(\omega_{1,M_0}-\omega_{2,M_0})-(\delta_{1,M_0}-\delta_{2,M_0})(\omega_{1,H_0}-\omega_{2,H_0})}\,p \tag{G1}$$

$$M_0=\frac{(\delta_{1,p}-\delta_{2,p})(\omega_{1,H_0}-\omega_{2,H_0})}{(\delta_{1,H_0}-\delta_{2,H_0})(\omega_{1,M_0}-\omega_{2,M_0})-(\delta_{1,M_0}-\delta_{2,M_0})(\omega_{1,H_0}-\omega_{2,H_0})}\,p \tag{G2}$$

where $\omega_{1,p}=\omega_{2,p}=0$. It is known from conventional membrane theory that the displacement perpendicular to the axis of symmetry of a point on the shell due to membrane forces only is

$$\overline{w}_p=\left(\frac{1-\nu}{2}\right)\frac{pR^2}{Eh}\sin\alpha\equiv\delta_p p \tag{G3a}$$

Since the membrane forces cause no rotation of the meridians,

$$\omega_p=0 \tag{G3b}$$

The other necessary edge influence coefficients can be found in equation (50).

With internal pressure and the discontinuity shear and moment in the directions shown, the edge influence coefficients are as given in the following equations:

$$\left.\begin{aligned}
&\delta_{1,p}=\frac{(1-\nu)R^2}{2Eh_1}\sin\alpha \qquad \delta_{2,p}=\frac{(1-\nu)R^2}{2Eh_2}\sin\alpha\\
&\delta_{1,H_0}=-\frac{2\lambda_2 R\sin^2\alpha}{Eh_1} \qquad \delta_{2,H_0}=\frac{2\lambda_2 R\sin^2\alpha}{Eh_2}\\
&\delta_{1,M_0}=\frac{2\lambda_1^2\sin\alpha}{Eh_1} \qquad \delta_{2,M_0}=\frac{2\lambda_2^2\sin\alpha}{Eh_2}\\
&\omega_{1,p}=0 \qquad \omega_{2,p}=0\\
&\omega_{1,H_0}=\frac{2\lambda_1^2\sin\alpha}{Eh_1} \qquad \omega_{2,H_0}=\frac{2\lambda_2^2\sin\alpha}{Eh_2}\\
&\omega_{1,M_0}=-\frac{4\lambda_1^3}{REh_1} \qquad \omega_{2,M_0}=\frac{4\lambda_2^3}{REh_2}
\end{aligned}\right\} \tag{G4}$$

If the influence coefficients of equations (G4) are substituted into equations (G1) and (G2), the equations for H_0 and M_0 take the form of equations (11) and (12) in the text.

APPENDIX H

SHEAR AND MOMENT AT THE JUNCTION OF A CYLINDER AND A CONE

In missile or space structures, a conical dome or bulkhead is usually attached to the main cylindrical body by means of a transition section such as a torus. However, there are applications where the cone is welded directly to the cylinder (fig. 5). For such cases, the discontinuity shear and moment at the junction are determined in the following paragraphs.

Let the subscript c refer to the cylinder and k to the cone. Positive shear and moment are as indicated in figure 5. From equations (E3) and (E4), the discontinuity shear and moment are determined as equations (14) and (15) in the text.

From membrane theory, the edge-displacement influence coefficient for the cylinder is

$$\delta_{c,p}=\left(1-\frac{\nu}{2}\right)\frac{a^2}{Eh_c} \tag{H1}$$

Since the meridian of a cylinder does not rotate because of membrane stresses, the edge-rotation influence coefficient is

$$\omega_{c,p}=0 \tag{H2}$$

The other necessary edge influence coefficients are given in equations (30) and (38), where the coefficients for the large end of the cone (subscript 1) are used. There are instances when the cylinder may be attached to the small end of the conical frustum. For this case, the coefficients for the small end of the conical frustum (subscript 2) should be used.

APPENDIX I

SHEAR AND MOMENT AT THE JUNCTION OF A CYLINDER AND A PORTION OF A SPHERE

The cylindrical pressure vessel is frequently closed at the ends by a portion of a sphere. The dome may subtend an angle considerably less than 180° (fig. 6(b)). The special case of a hemispherical dome as the closure (fig. 6(c)) is commonly used. The equations given here are also applicable to the case of a subtended angle in the dome greater than 180° (fig. 6(d)). The restrictions imposed upon the spherical shell in appendix C apply here also. The discontinuity shear and moment at the junction of the cylinder and spherical dome are determined in the following paragraphs. Positive shear and moment are as shown in figure 6(a).

With the subscript c referring to the cylinder and s to the portion of a sphere, the following equations express the edge rotation and deflection of the two shells at their junction:

$$\left.\begin{aligned} \overline{w}_{0,c} &= \delta_{c,H_0}H_0+\delta_{c,M_0}M_0+\delta_{c,p}p \\ V_{0,c} &= \omega_{c,H_0}H_0+\omega_{c,M_0}M_0+\omega_{c,p}p \\ \overline{w}_{0,s} &= \delta_{s,H_0}\left(H_0+\frac{pR}{2}\cos\alpha\right)+\delta_{s,M_0}M_0+\delta_{s,p}p \\ V_{0,s} &= \omega_{s,H_0}\left(H_0+\frac{pR}{2}\cos\alpha\right)+\omega_{s,M_0}M_0+\omega_{s,p}p \end{aligned}\right\} \quad (I1)$$

Continuity of rotation and deflection at the junction requires

$$\left.\begin{aligned} V_{0,c} &= V_{0,s} \\ \overline{w}_{0,c} &= \overline{w}_{0,s} \end{aligned}\right\} \quad (I2)$$

Substituting equations (I1) into (I2) gives

$$\begin{aligned} H_0 = \Bigg\{ &\left[\omega_{s,H_0}(\delta_{c,M_0}-\delta_{s,M_0})-\delta_{s,H_0}(\omega_{c,M_0}-\omega_{s,M_0})\right]\frac{R}{2}\cos\alpha \\ &+(\delta_{c,p}-\delta_{s,p})\,(\omega_{c,M_0}-\omega_{s,M_0})-(\delta_{c,M_0}-\delta_{s,M_0})\,(\omega_{c,p}-\omega_{s,p})\Bigg\}p \\ &\div\left[(\delta_{c,M_0}-\delta_{s,M_0})\,(\omega_{c,H_0}-\omega_{s,H_0})-(\delta_{c,H_0}-\delta_{s,H_0})\,(\omega_{c,M_0}-\omega_{s,M_0})\right] \end{aligned} \quad (I3)$$

and

$$M_0=\frac{(\delta_{s,H_0}\omega_{c,H_0}-\delta_{c,H_0}\omega_{s,H_0})\frac{R}{2}\cos\alpha+(\delta_{c,H_0}-\delta_{s,H_0})(\omega_{c,p}-\omega_{s,p})-(\delta_{c,p}-\delta_{s,p})(\omega_{c,H_0}-\omega_{s,H_0})}{(\delta_{c,M_0}-\delta_{s,M_0})(\omega_{c,H_0}-\omega_{s,H_0})-(\delta_{c,H_0}-\delta_{s,H_0})(\omega_{c,M_0}-\omega_{s,M_0})}p \quad (I4)$$

The edge coefficients for the membrane stresses are

$$\left.\begin{aligned} \delta_{c,p} &= \left(1-\frac{\nu}{2}\right)\frac{a^2}{Eh_c} & \delta_{s,p} &= \frac{(1-\nu)R^2\sin\alpha}{2Eh_s} \\ \omega_{c,p} &= 0 & \omega_{s,p} &= 0 \end{aligned}\right\} \quad (I5)$$

The remaining edge influence coefficients are obtained from equations (30) and (50). Substitution of the edge coefficients into equations (I3) and (I4) results in equations (17) and (18) in the text.

APPENDIX J

SHEAR AND MOMENT AT THE JUNCTION OF A CYLINDER AND A FLAT HEAD

One of the simplest closures for a cylindrical pressure vessel is the flat plate head. This is a very stiff restraint on the cylinder and therefore induces stresses in the cylinder higher than would be produced by most of the other closures. However, since it is the easiest and cheapest to fabricate, it is sometimes used in experimental facilities or for other such purposes where the weight of the vessel is not critical or where the higher induced stresses can be tolerated.

The discontinuity shear and moment are determined here for this case with the sign convention being as shown in figure 7. Let the subscript c refer to the cylinder and f to the flat plate. With

$$\omega_{c,p}=\delta_{f,M_0}=\delta_{f,p}=\omega_{f,H_0}=0 \tag{J1}$$

equations (E3) and (E4) become

$$H_0=\frac{-\delta_{c,M_0}\omega_{f,p}-\delta_{c,p}(\omega_{c,M_0}-\omega_{f,M_0})}{(\delta_{c,H_0}-\delta_{f,H_0})(\omega_{c,M_0}-\omega_{f,M_0})-\delta_{c,M_0}\omega_{c,H_0}}p \tag{J2}$$

and

$$M_0=\frac{\delta_{c,p}\omega_{c,H_0}+\omega_{f,p}(\delta_{c,H_0}-\delta_{f,H_0})}{(\delta_{c,H_0}-\delta_{f,H_0})(\omega_{c,M_0}-\omega_{f,M_0})-\delta_{c,M_0}\omega_{c,H_0}}p \tag{J3}$$

Substituting the expressions for the edge influence coefficients found in equations (16), (30), and (56) into equations (J2) and (J3) yields equations (20) and (21) in the text. Having found the desired discontinuity shear and moment, the stresses in the cylinder and plate can now be computed.

APPENDIX K

SHEAR AND MOMENT AT THE JUNCTION OF A CONE AND A PORTION OF A SPHERE

The toriconical head is frequently used in tank design. The special case in which the torus is a portion of a sphere (fig. 13) can be analyzed in the following manner. Because the expansions of the cone and the portion of a sphere due to membrane stresses only are not, in general, the same at the junction, discontinuity forces must be present to make the rotations and deflections identical at their common boundary.

Assume positive shear and moment to be in the directions shown in figure 8. The rotation and deflection at the junction of the cone and the portion of a sphere can be expressed in terms of edge influence coefficients, discontinuity shear and moment, and internal pressure. The equations expressing the relations can be written as follows:

$$\left.\begin{aligned}
\overline{w}_{0,k}&=\delta_{k,H_0}H_0+\delta_{k,M_0}M_0+\delta_{k,p}p\\
V_{0,k}&=\omega_{k,H_0}H_0+\omega_{k,M_0}M_0+\omega_{k,p}p\\
\overline{w}_{0,s}&=\delta_{s,H_0}\left(H_0+\frac{pR_s}{2}\cos\alpha_s\right)+\delta_{s,M_0}M_0+\delta_{s,p}p\\
V_{0,s}&=\omega_{s,H_0}\left(H_0+\frac{pR_s}{2}\cos\alpha_s\right)+\omega_{s,M_0}M_0+\omega_{s,p}p
\end{aligned}\right\} \quad \text{(K1)}$$

The subscripts k and s refer to the cone and spherical shell, respectively. Continuity of rotation and deflection at the junction results in the following equations:

$$\left.\begin{aligned}
V_{0,k}&=V_{0,s}\\
\overline{w}_{0,k}&=\overline{w}_{0,s}
\end{aligned}\right\} \quad \text{(K2)}$$

Substitution of equations (K1) into equations (K2) gives equations (23) and (24) in the text. The edge influence coefficients are obtained from equations (38) and (50). Note the changes in the signs of some influence coefficients, as mentioned in the body of the report. In addition, the coefficient $\omega_{s,p}$ is zero, since the meridians of a sphere do not rotate when subjected to membrane stresses only. The edge-displacement coefficient for the portion of the sphere due to internal pressure $\delta_{s,p}$ can readily be obtained from membrane theory. The expressions for $\omega_{s,p}$ and $\delta_{s,p}$ are then

$$\left.\begin{aligned}
\omega_{s,p}&=0\\
\text{and}\qquad \delta_{s,p}&=\frac{1-\nu}{2}\frac{R_s^2}{Eh_s}\sin\alpha_s
\end{aligned}\right\} \quad \text{(K3)}$$

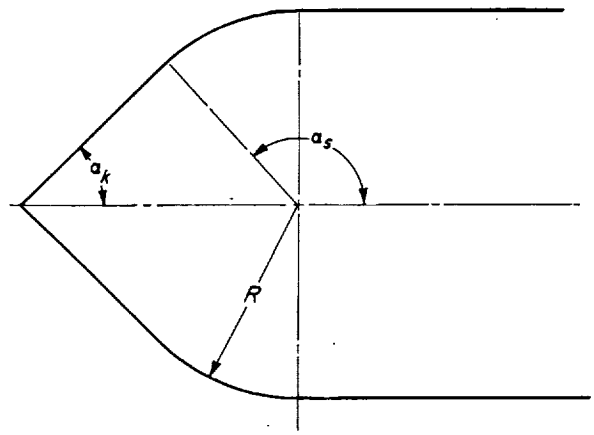

FIGURE 13.—Toriconical head on cylinder.

APPENDIX L

EFFECT OF NONCONCURRENCE OF MIDDLE SURFACES AT SHELL JUNCTIONS

Frequently the middle surfaces of two shells do not coincide at their junction. This situation may arise because the shell has been milled on only one surface or because two shells of different thicknesses have been joined to give a smooth outer contour or for some other reason. This eccentricity of the middle surfaces induces bending stresses in addition to those previously found for the shell junctions which have continuous middle surfaces. The following paragraphs show how these additional bending stresses can be found.

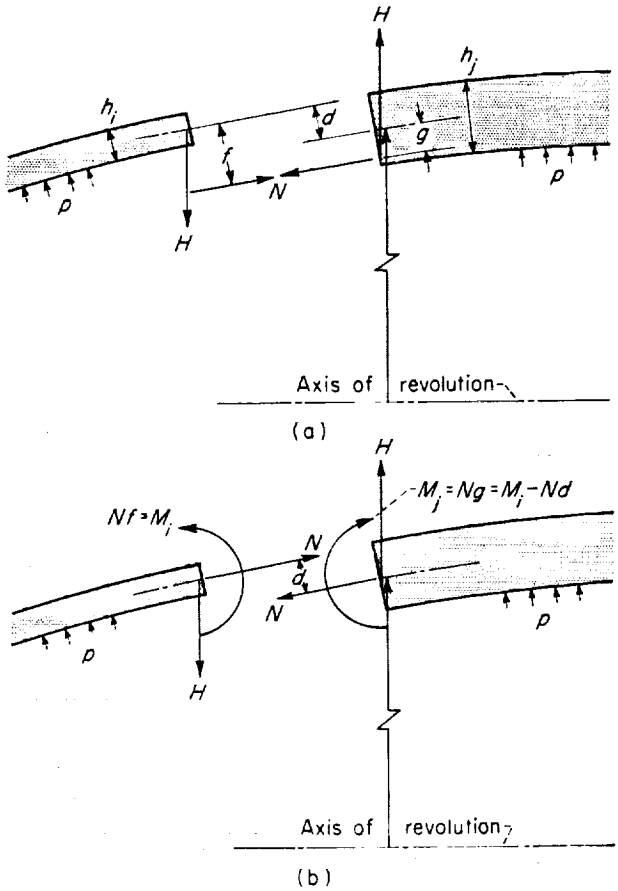

(a) Fundamental force system.
(b) Conventional force system.

FIGURE 14.—Shell junction with nonconcurrent middle surfaces.

Consider first the case where the tangents to the meridians at the shell junction are parallel. Let the meridional membrane force be denoted by N and the distance normal to the shell between the middle surfaces be d as shown in figure 14(a). As before, imagine the shell to be cut into two pieces by a plane passing through the junction. Very fundamentally, it is possible to represent the forces at the cut by equal and opposite shear forces H and equal, opposite, and colinear normal forces N acting along some unknown line of action. Assume this line of action is at distances f and g from the middle surfaces of shells i and j, respectively. Since N represents the resultant meridional force on either side of the cut, there is no bending moment present. The meridional forces are moved to the middle surfaces along with bending moments Nf and Ng as shown. Notice that the moments acting on the two edges are not equal. This is a result of the nonconcurrence of the middle surfaces and the fact that the meridional forces N are not now colinear. Let

$$M_i = Nf \tag{L1}$$

Then, considering only the geometry, the moment on the other side of the junction is

$$M_j = Ng = M_i - Nd \tag{L2}$$

The equations of continuity at the junction are

$$\left.\begin{aligned} V_{0,i} &= V_{0,j} \\ \overline{w}_{0,i} &= \overline{w}_{0,j} \end{aligned}\right\} \tag{L3}$$

In terms of edge influence coefficients, edge loads and internal pressure, equation (L3) becomes

$$\left.\begin{aligned} \omega_{i,H}H + \omega_{i,M}M_i + \omega_{i,p}p &= \omega_{j,H}H + \omega_{j,M}M_j + \omega_{j,p}p \\ \delta_{i,H}H + \delta_{i,M}M_i + \delta_{i,p}p &= \delta_{j,H}H + \delta_{j,M}M_j + \delta_{j,p}p \end{aligned}\right\} \tag{L4}$$

Substituting equation (L2) into (L4) and solving for H and M_i yield

$$H=\frac{(\omega_{i,M}-\omega_{j,M})(\delta_{i,p}-\delta_{j,p})-(\omega_{i,p}-\omega_{j,p})(\delta_{i,M}-\delta_{j,M})}{(\omega_{i,H}-\omega_{j,H})(\delta_{i,M}-\delta_{j,M})-(\omega_{i,M}-\omega_{j,M})(\delta_{i,H}-\delta_{j,H})}\,p$$

$$+\frac{\omega_{i,M}\delta_{j,M}-\omega_{j,M}\delta_{i,M}}{(\omega_{i,H}-\omega_{j,H})(\delta_{i,M}-\delta_{j,M})-(\omega_{i,M}-\omega_{j,M})(\delta_{i,H}-\delta_{j,H})}\,Nd \quad \text{(L5)}$$

$$M_i=\frac{(\omega_{i,p}-\omega_{j,p})(\delta_{i,H}-\delta_{j,H})-(\omega_{i,H}-\omega_{j,H})(\delta_{i,p}-\delta_{j,p})}{(\omega_{i,H}-\omega_{j,H})(\delta_{i,M}-\delta_{j,M})-(\omega_{i,M}-\omega_{j,M})(\delta_{i,H}-\delta_{j,H})}\,p$$

$$+\frac{\omega_{j,M}(\delta_{i,H}-\delta_{j,H})-(\omega_{i,H}-\omega_{j,H})\delta_{j,M}}{(\omega_{i,H}-\omega_{j,H})(\delta_{i,M}-\delta_{j,M})-(\omega_{i,M}-\omega_{j,M})(\delta_{i,H}-\delta_{j,H})}\,Nd \quad \text{(L6)}$$

Substitution of equation (L6) into (L2) gives

$$M_j=\frac{(\omega_{i,p}-\omega_{j,p})(\delta_{i,H}-\delta_{j,H})-(\omega_{i,H}-\omega_{j,H})(\delta_{i,p}-\delta_{j,p})}{(\omega_{i,H}-\omega_{j,H})(\delta_{i,M}-\delta_{j,M})-(\omega_{i,M}-\omega_{j,M})(\delta_{i,H}-\delta_{j,H})}\,p$$

$$+\frac{\omega_{i,M}(\delta_{i,H}-\delta_{j,H})-(\omega_{i,H}-\omega_{j,H})\delta_{i,M}}{(\omega_{i,H}-\omega_{j,H})(\delta_{i,M}-\delta_{j,M})-(\omega_{i,M}-\omega_{j,M})(\delta_{i,H}-\delta_{j,H})}\,Nd \quad \text{(L7)}$$

The first parts of equations (L5) to (L7) are recognized to be the discontinuity forces determined before when the middle surfaces were continuous (see eqs. (E3) and (E4)). The other terms are the effect of the nonconcurrence of the middle surfaces. Thus the discontunity forces due to only the nonconcurrence of the middle surfaces can be computed by using the second half of equations (L5) to (L7). These forces can then be added to those given in the body of the report to obtain the resultant stress distribution.

The sign of the bending moment Nd must be assigned with care. It would be oppositely directed if the middle surface of shell i were inside the middle surface of shell j at the junction (fig. 14(b)).

If the tangents to the meridians at the shell junction are not parallel, it is not possible to use the foregoing equations because the meridional forces are not equal and opposite. In such a case, it is probably most convenient to work with forces at the junction which are either parallel or perpendicular to the shell axis. As in the previous analysis, the components perpendicular to the shell axis do not affect the edge moment. In computing the bending moments due to nonconcurrence of the middle surfaces in this case, the eccentricity of the middle surfaces must be measured normal to the shell axis. Equations similar to (L5) to (L7) will finally result. Because of the lack of availability of all necessary influence coefficients, this case was not pursued further.

REFERENCES

1. Taylor, Charles E., and Wenk, Edward, Jr.: Analysis of Stress in the Conical Elements of Shell Structures. Rep. 981, David W. Taylor Model Basin, May 1956.
2. Lowell, Herman H.: Tables of the Bessel-Kelvin Functions *ber*, *bei*, *ker*, *kei*, and Their Derivatives for the Argument Range 0(0.01) 107.50. NASA TR R-32, 1959.
3. Timoshenko, S., and Woinowsky-Krieger, S.: Theory of Plates and Shells. Second ed., McGraw-Hill Book Co., Inc., 1959.
4. Hetényi, M.: Beams on Elastic Foundation. Univ. of Mich. Press, 1946.
5. Hoff, Nicholas J.: General Formulas for Influence Coefficients for Thin Spherical Shells. Paper 61-15, Inst. Aero. Sci., 1961.
6. Reissner, Eric: Stresses and Small Displacements of Shallow Spherical Shells, pt. I, Jour. Math. Phys., vol. 25, no. 1, Feb. 1946, pp. 80–85.
7. Baltrukonis, J. H.: Influence Coefficients for Edge-Loaded Short, Thin, Conical Frustums. Jour. Appl. Mech., vol. 26, no. 3, June 1959, pp. 241–245.
8. Watts, G. W., and Burrows, W. R.: The Basic Elastic Theory of Vessel Heads Under Internal Pressure. Jour. Appl. Mech., vol. 16, no. 1, Mar. 1949, pp. 55–73.

U.S. GOVERNMENT PRINTING OFFICE: 1961